Supersymmetric grand unified theories: Two-loop evolution of gauge and Yukawa couplings

V. Barger, M. S. Berger, and P. Ohmann
Physics Department, University of Wisconsin, Madison, Wisconsin 53706
(Received 14 September 1992)

We make a numerical study of gauge and Yukawa unification in supersymmetric grand unified models and examine the quantitative implications of fermion mass *Ansätze* at the grand unified scale. Integrating the renormalization group equations with $\alpha_1(M_Z)$ and $\alpha_2(M_Z)$ as inputs, we find $\alpha_3(M_Z) \simeq 0.111(0.122)$ for $M_{\rm SUSY} = m_t$ and $\alpha_3(M_Z) \simeq 0.106(0.116)$ for $M_{\rm SUSY} = 1$ TeV at one-loop (two-loop) order. Including b and τ Yukawa couplings in the evolution, we find an upper limit of $m_t \lesssim 200$ GeV from Yukawa unification. For given $m_t \lesssim 175$ GeV, there are two solutions for β: one with $\tan\beta > m_t/m_b$, and one with $\sin\beta \simeq 0.78(m_t/150\ {\rm GeV})$. Taking a popular *Ansatz* for the mass matrices at the unified scale, we obtain a lower limit on the top-quark mass of $m_t \gtrsim 150(115)$ GeV for $\alpha_3(M_Z) = 0.11(0.12)$ and an upper limit on the supersymmetry parameter $\tan\beta \lesssim 50$ if $\alpha_3(M_Z) = 0.11$. The evolution of the quark mixing matrix elements is also evaluated.

PACS number(s): 12.10.Dm, 12.15.Ff

I. INTRODUCTION

There is renewed interest in supersymmetric grand unified theories (GUT's) [1] to explain gauge couplings, fermion masses, and quark mixings [2–9]. Recent measurements of the gauge couplings at the CERN e^+e^- collider LEP and in other low-energy experiments [10, 11] are in reasonably good accord with expectations from minimal supersymmetric GUT's with the scale of supersymmetry (SUSY) of order 1 TeV or below [2]. Supersymmetric GUT's are also consistent with the nonobservation to date of proton decay [12]. In addition to the unification of gauge couplings [13], the unification of Yukawa couplings has been considered to predict relations among quark masses [14–16]. With equal b-quark and τ-lepton Yukawa couplings at the GUT scale, the m_b/m_τ mass ratio is explained by SUSY GUT's [4, 15]. With specific *Ansätze* for the GUT-scale mass matrices (e.g., zero elements, mass hierarchy, relations of quark and lepton elements), other predictions have been obtained from quark masses and mixings that are consistent with measurements [4, 6, 7, 17, 18]. The consideration of fermion mass relationships has a long history [19–21] and includes single relations and mass matrices ("textures") without evolution [22–24], and single relations and mass matrices with evolution [25].

Our approach is to explore supersymmetric GUT's first with the most general assumptions, and then proceed to add additional GUT unification constraints to obtain more predictions at the electroweak scale. The renormalization-group equations (RGE's) used here are for the supersymmetric GUT's [26, 27] with the minimal particle content above the supersymmetry scale and the standard model RGE's [28] below the supersymmetry scale. In Sec. II we explore the running of the gauge couplings in the supersymmetric model at the two-loop level and compare the results to those obtained at the one-loop level. Rather than try to predict the scale of supersymmetry ($M_{\rm SUSY}$) which may be sensitive to unknown and model-dependent effects such as particle thresholds at the GUT scale, we choose two values of $M_{\rm SUSY}$ to illustrate the general trends that occur. We also investigate the effects of the Yukawa couplings on the gauge coupling running, which enter at two loops [17] and have often been neglected in the past. In Sec. III we explore the unification of Yukawa coupling constants. First we consider the one-loop analytic solutions which can be obtained by neglecting the bottom-quark and τ Yukawa couplings λ_b and λ_τ relative to λ_t in the RGE's. This serves as a useful standard for comparison with the two-loop results for smaller values of $\tan\beta$ ($\ll m_t/m_b$), and many of the general features of the solutions to the RGE's are already present at this stage. We then investigate the two-loop RGE evolution of the Yukawa couplings including the effects of λ_b, λ_τ, and λ_t. Analytic solutions are not available for the two-loop evolution, so we integrate the RGE's numerically. In Sec. IV we investigate relations between Cabibbo-Kobayashi-Maskawa (CKM) matrix elements and the ratios of quark masses. We investigate two popular *Ansätze* [6, 7, 16] for Yukawa coupling matrices at the GUT scale. Both of these *Ansätze* agree with all existing experimental data, and this agreement is preserved at the two-loop level. We also integrate the two-loop evolution equations for certain CKM matrix elements and quark mass ratios in Sec. IV. The two-loop RGE's for both the minimal supersymmetric model and the standard model are given in the appendix.

II. GAUGE COUPLING UNIFICATION

A consistent treatment to two loops in the running of the gauge couplings involves the gauge couplings g_i and the largest Yukawa couplings λ_t, λ_b and λ_τ. From general expressions [26, 27] that are summarized in the Appendix, we obtain the evolution equations

$$\frac{dg_i}{dt} = \frac{g_i}{16\pi^2}\left[b_i g_i^2 + \frac{1}{16\pi^2}\left(\sum_{j=1}^{3} b_{ij} g_i^2 g_j^2 - \sum_{j=t,b,\tau} a_{ij} g_i^2 \lambda_j^2\right)\right] , \tag{1}$$

$$\begin{aligned}\frac{d\lambda_t}{dt} = \frac{\lambda_t}{16\pi^2}\Bigg[& \left(-\sum c_i g_i^2 + 6\lambda_t^2 + \lambda_b^2 \right) \\ & + \frac{1}{16\pi^2}\Bigg(\sum \left(c_i b_i + c_i^2/2\right) g_i^4 + g_1^2 g_2^2 + \frac{136}{45} g_1^2 g_3^2 + 8 g_2^2 g_3^2 \\ & + \lambda_t^2 \left(\frac{6}{5} g_1^2 + 6 g_2^2 + 16 g_3^2\right) + \frac{2}{5}\lambda_b^2 g_1^2 - \left\{22\lambda_t^4 + 5\lambda_t^2\lambda_b^2 + 5\lambda_b^4 + \lambda_b^2\lambda_\tau^2\right\} \Bigg)\Bigg] ,\end{aligned} \tag{2}$$

$$\begin{aligned}\frac{d\lambda_b}{dt} = \frac{\lambda_b}{16\pi^2}\Bigg[& \left(-\sum c_i' g_i^2 + \lambda_t^2 + 6\lambda_b^2 + \lambda_\tau^2 \right) \\ & + \frac{1}{16\pi^2}\Bigg(\sum \left(c_i' b_i + c_i'^2/2\right) g_i^4 + g_1^2 g_2^2 + \frac{8}{9} g_1^2 g_3^2 + 8 g_2^2 g_3^2 + \frac{4}{5}\lambda_t^2 g_1^2 + \lambda_b^2 \left(\frac{2}{5} g_1^2 + 6 g_2^2 + 16 g_3^2\right) + \frac{6}{5}\lambda_\tau^2 g_1^2 \\ & - \left\{22\lambda_b^4 + 5\lambda_t^2\lambda_b^2 + 3\lambda_b^2\lambda_\tau^2 + 3\lambda_\tau^4 + 5\lambda_t^4\right\} \Bigg)\Bigg] ,\end{aligned} \tag{3}$$

$$\begin{aligned}\frac{d\lambda_\tau}{dt} = \frac{\lambda_\tau}{16\pi^2}\Bigg[& \left(-\sum c_i'' g_i^2 + 3\lambda_b^2 + 4\lambda_\tau^2 \right) \\ & + \frac{1}{16\pi^2}\Bigg(\sum \left(c_i'' b_i + c_i''^2/2\right) g_i^4 + \frac{9}{5} g_1^2 g_2^2 \\ & + \lambda_b^2 \left(-\frac{2}{5} g_1^2 + 16 g_3^2\right) + \lambda_\tau^2 \left(\frac{6}{5} g_1^2 + 6 g_2^2\right) - \left\{3\lambda_t^2\lambda_b^2 + 9\lambda_b^4 + 9\lambda_b^2\lambda_\tau^2 + 10\lambda_\tau^4\right\} \Bigg)\Bigg] .\end{aligned} \tag{4}$$

The various coefficients in the above expressions are also given in the Appendix. The variable is $t = \ln(\mu/M_G)$ where μ is the running mass scale and M_G is the GUT unification mass. The renormalization-group equations of dimensionless parameters such as the gauge couplings and Yukawa couplings are independent of the dimensionful soft-supersymmetry-breaking parameters.

We begin with the recent values of $\alpha_{\rm em}$ and $\sin^2\hat{\theta}_W$ at scale $M_Z = 91.17$ GeV given by the 1992 Particle Data Group [11, 29]

$$(\alpha_{\rm em})^{-1} = 127.9 \pm 0.2 , \tag{5a}$$

$$\sin^2\hat{\theta}_W = 0.2326 \pm 0.0008 , \tag{5b}$$

where $\hat{\theta}_W$ refers to the weak angle in the modified minimal subtraction ($\overline{\rm MS}$) scheme [30]. These values correspond to electroweak gauge couplings of

$$\alpha_1(M_Z)^{-1} = 58.89 \pm 0.11 , \tag{6a}$$

$$\alpha_2(M_Z)^{-1} = 29.75 \pm 0.11 . \tag{6b}$$

For simplicity we initially set the supersymmetric scale $M_{\rm SUSY}$ equal to the top-quark mass m_t and set all Yukawa contributions in Eq. (1) to zero. Then evolving α_1 and α_2 from scale M_Z up to scale m_t, we have

$$\alpha_1(m_t)^{-1} = \alpha_1(M_Z)^{-1} + \frac{53}{30\pi}\ln(M_Z/m_t) , \tag{7a}$$

$$\alpha_2(m_t)^{-1} = \alpha_2(M_Z)^{-1} - \frac{11}{6\pi}\ln(M_Z/m_t) . \tag{7b}$$

We use the value $M_Z = 91.17$ GeV, neglecting its experimental uncertainty.

Next, for a grid of α_G and M_G values, we evolve from the GUT scale down to the chosen m_t scale and retain those GUT scale inputs for which Eqs. (6) and (7) are satisfied. We use the two-loop SUSY GUT unification condition $\alpha_G = \alpha_1(M_G) = \alpha_2(M_G)$. For the acceptable GUT inputs we also evolve the strong coupling $\alpha_3(M_G) = \alpha_G$ down to scale m_t and then use three-loop QCD to further evolve it to scale M_Z. The three-loop expression

$$\alpha_3(\mu)^{-1} = -\frac{b_0}{2}\ln\left(\frac{\mu^2}{\Lambda^2}\right) + \frac{b_1}{b_0}\ln\left(\ln\frac{\mu^2}{\Lambda^2}\right) - 2\frac{b_1^2}{b_0^3}\left[\ln\left(\ln\frac{\mu^2}{\Lambda^2}\right) - \left(\frac{b_0 b_2}{b_1^2} - 1\right)\right]\left(\ln\frac{\mu^2}{\Lambda^2}\right)^{-1} , \tag{8}$$

with the b_i given in Ref. [31], is iteratively solved to find Λ from $\alpha_3(m_t)$. Equation (8) is then evaluated for $\mu = M_Z$ to obtain $\alpha_3(M_Z)$. The resulting values for Λ for two representative values of $\alpha_3(M_Z)$ are given in Table I.

We also investigate the effects of taking a supersymmetry scale higher than m_t. Below $M_{\rm SUSY}$, the RGE's are similar to the nonsupersymmetric standard model. A linear combination of the Higgs doublets is integrated out of the theory at $M_{\rm SUSY}$ leaving the orthogonal combination $\Phi_{\rm (SM)} = \Phi_d \cos\beta + \tilde{\Phi}_u \sin\beta$ coupled to the fermions in a way that depends on $\tan\beta$ [4, 32, 33]; this combination results from the assumption that the three soft-supersymmetry breaking parameters in the Higgs potential can be equated to $M_{\rm SUSY}$. We use the two-loop RGE's [28] for the standard model, matching the couplings at $M_{\rm SUSY}$. Taking a single SUSY scale is an idealized situation since in general the supersymmetric particle spectrum is spread over a range of masses [9]. Without further assumptions we cannot predict this spectrum. Given that such uncertainties exist, the predicted range for α_3 should be taken to be representative only.

The ranges of α_G^{-1} and M_G parameters obtained from the procedure outlined above are presented in Fig. 1 for one-loop and two-loop evolution with the choices $M_{\rm SUSY} = m_t$ and $M_{\rm SUSY} = 1$ TeV. The shaded regions denote the allowed GUT parameter space. The two-loop values obtained for α_G and M_G are higher than the one-loop values and consequently $\alpha_3(M_Z)$ is higher for the two-loop evolution. Note that raising the SUSY scale from m_t to 1 TeV lowers M_G and α_G; hence $\alpha_3(M_Z)$ decreases as well.

Figure 2 shows the corresponding results of the two-loop evolution over the full range of μ. We find the ranges for $\alpha_3(M_Z)$ with $m_t = 150$ GeV shown in Table II. The two-loop values of $\alpha_3(M_Z)$ are about 10% larger than the one-loop values. The effect of the higher SUSY scale is to lower $\alpha_3(M_Z)$ by about 5%.

TABLE I. The QCD parameter $\Lambda^{(n_f)}$ in MeV, where n_f is the number of active flavors.

$\alpha_3(M_Z)$	$\Lambda^{(5)}$	$\Lambda^{(4)}$	$\Lambda^{(3)}$
0.11	129.1	188.3	225.0
0.12	233.4	320.2	360.0

Inclusion of Yukawa couplings in the two-loop evolution also lowers the value of $\alpha_3(M_Z)$ somewhat. For example setting $\lambda_t = \lambda_b = \lambda_\tau = 1$ at the GUT scale, we obtain a two-loop value of $\alpha_3(M_Z) = 0.1189 \pm 0.0031$ for $M_{\rm SUSY} = m_t$.

The effects on the gauge couplings of including the Yukawa couplings in the evolution are rather small for Yukawa couplings in the perturbative regime, justifying their neglect in most previous analyses; for large values of $\tan\beta$ the changes in the gauge couplings due to inclusion of Yukawa couplings can be a few percent.

The experimental situation regarding the determination of α_3 is presently somewhat clouded [10], with deep inelastic scattering determinations in the range of the one-loop calculations in Table II and LEP determinations similar to the two-loop results of Table II.

There are other uncertainties not taken into account here, due to threshold corrections from the unknown particle content at the heavy scale [34–36], which can also change the α_3 values obtained above. These corrections are model dependent so we have not attempted to include such contributions. However, recent analysis have shown that the constraints from nonobservation of proton decay greatly reduce the potential uncertainties from GUT thresholds [17, 37].

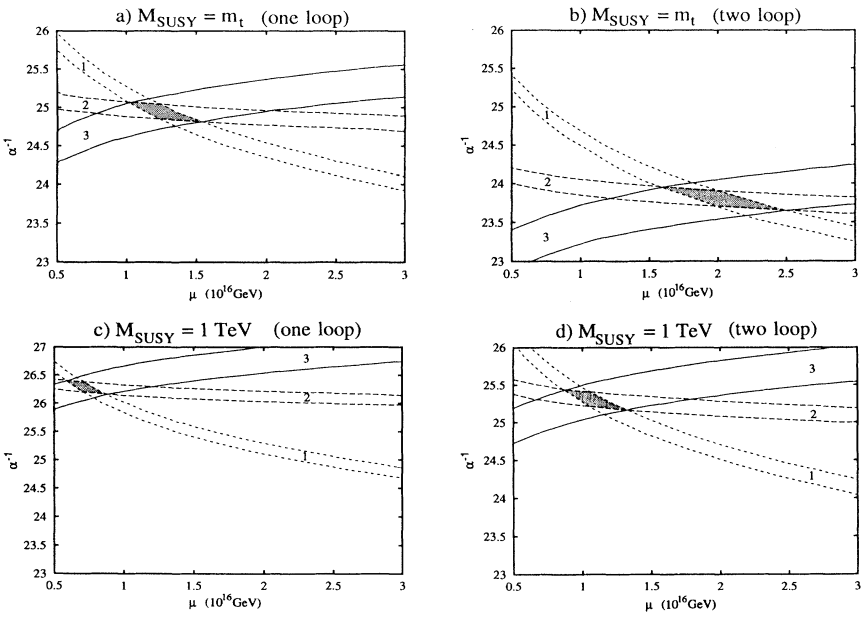

FIG. 1. Allowed GUT parameter space for running top-quark mass $m_t = 150$ GeV with (a) $M_{\rm SUSY} = m_t$ (one-loop RGE), (b) $M_{\rm SUSY} = m_t$ (two-loop RGE), (c) $M_{\rm SUSY} = 1$ TeV (one-loop RGE), (d) $M_{\rm SUSY} = 1$ TeV (two-loop RGE) versus the running mass scale μ. The shaded region denotes the range of GUT coupling and mass consistent with the 1σ ranges of $\alpha_1(M_Z)$ and $\alpha_2(M_Z)$; the curves for $\alpha_3(\mu)$ represent extrapolations from the GUT parameters. We have omitted the contributions from Yukawa effects here which depend on $\tan\beta$.

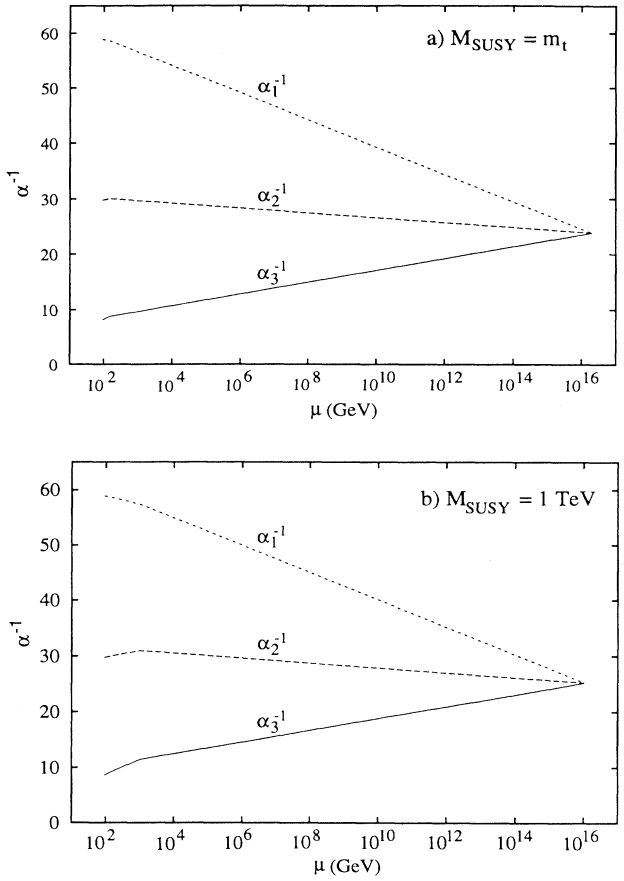

FIG. 2. Gauge coupling unification with two-loop evolution for (a) $M_{\rm SUSY} = m_t$, (b) $M_{\rm SUSY} = 1$ TeV, taking $m_t = 150$ GeV and neglecting Yukawa couplings; μ is the running mass scale.

TABLE II. Ranges obtained for $\alpha_3(M_Z)$ from the input values $\alpha_{\rm em}$ and $\sin^2\hat{\theta}_W$.

$M_{\rm SUSY}$	One loop	Two loop
$m_t = 150$ GeV	0.1112 ± 0.0024	0.1224 ± 0.0033
1 TeV	0.1065 ± 0.0024	0.1161 ± 0.0028

III. YUKAWA UNIFICATION

A. One-loop analytic results

The unification of Yukawa couplings first introduced by Chanowitz, Ellis, and Gaillard [14] has been reconsidered recently [4, 6, 7, 17, 32]. The GUT-scale condition $\lambda_b(M_G) = \lambda_\tau(M_G)$ leads to a successful prediction for the mass ratio m_b/m_τ provided that a low-energy supersymmetry exists [4]. The b to τ mass ratio is given by

$$\frac{m_b}{m_\tau} = \frac{\eta_b}{\eta_\tau} R_{b/\tau}(m_t) \,, \tag{9}$$

where

$$R_{b/\tau}(m_t) \equiv \frac{\lambda_b(m_t)}{\lambda_\tau(m_t)} = \frac{m_b(m_t)}{m_\tau(m_t)} \,, \tag{10}$$

is the b to τ ratio of running masses at scale m_t and

$$\eta_f = \frac{m_f(m_f)}{m_f(m_t)} \qquad \text{if} \quad m_f > 1 \text{ GeV} \,, \tag{11}$$

$$\eta_f = \frac{m_f(1\text{GeV})}{m_f(m_t)} \qquad \text{if} \quad m_f < 1 \text{ GeV} \,, \tag{12}$$

is a scaling factor including both QCD and QED effects in the running mass below m_t. We have determined the η_f scaling factors to three-loop order in QCD and one-loop order in QED. The QCD running of the quark mass is described by

$$m_q(\mu) = \hat{m}_q \, (2b_0\alpha_3)^{\gamma_0/b_0} \left\{ 1 + \left(\frac{\gamma_1}{b_0} - \frac{\gamma_0 b_1}{b_0^2} \right) \alpha_3 + \frac{1}{2} \left[\left(\frac{\gamma_1}{b_0} - \frac{\gamma_0 b_1}{b_0^2} \right)^2 + \left(\frac{\gamma_2}{b_0} + \frac{\gamma_0 b_1^2}{b_0^3} - \frac{b_1\gamma_1 + b_2\gamma_0}{b_0^2} \right) \right] \alpha_3^2 + \mathcal{O}(\alpha_3^3) \right\} \,, \tag{13}$$

where the anomalous dimensions γ_0, γ_1, and γ_2 are given in Ref. [38]. The scale-invariant mass $\hat{m}_q$ cancels in the ratio in Eq. (11). The one-loop QED running from scale μ' to scale μ introduces modifications

$$m_f(\mu) = m_f(\mu') \left(\frac{\alpha(\mu)}{\alpha(\mu')} \right)^{\gamma_0^{\rm QED}/b_0^{\rm QED}} \,, \tag{14}$$

where the QED β function and anomalous dimension are given by [35]

$$b_0^{\rm QED} = \frac{4}{3} \left(3 \sum Q_u^2 + 3 \sum Q_d^2 + \sum Q_e^2 \right) \,, \tag{15}$$

$$\gamma_0^{\rm QED} = -3Q_f^2 \,, \tag{16}$$

and the sums run over the active fermions at the relevant scale. The dependence of the QCD-QED scaling factors η on $\alpha_3(M_Z)$ is shown in Fig. 3; these factors increase as $\alpha_3(M_Z)$ increases.

We note that the physical top-quark mass is related to the running mass by [39]

$$m_t^{\rm phys} = m_t(m_t) \left[1 + \frac{4}{3\pi} \alpha_3(m_t) + O(\alpha_3^2) \right] \,. \tag{17}$$

Throughout this paper we use m_t and m_b to denote the running mass values $m_t(m_t)$ and $m_b(m_b)$.

The effects of the top-quark Yukawa coupling λ_t can be studied semianalytically at one loop neglecting the effects of the bottom and tau Yukawa couplings λ_b and λ_τ in Eqs. (1) and (2), which is a valid approximation for small to moderate $\tan\beta$ (i.e., $\tan\beta \lesssim 10$). Following Ref. [6] we find [40]

$$\frac{m_b}{m_\tau} = y \frac{\eta^{1/2}}{x} \frac{\eta_b}{\eta_\tau} \,, \tag{18}$$

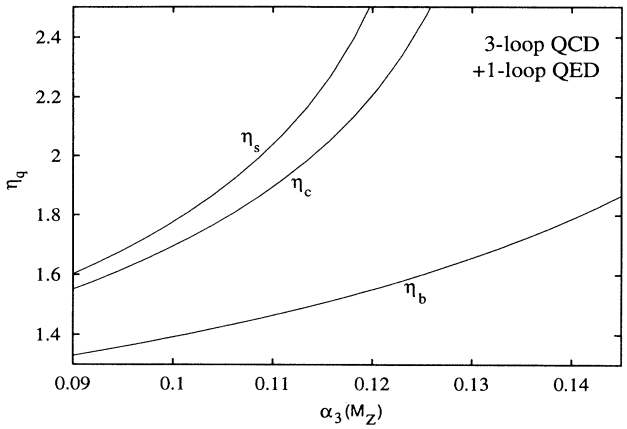

FIG. 3. The QCD-QED scaling factors η_f of Eq. (11) are shown for $f = s, c, b$ versus $\alpha_3(M_Z)$, assuming running quark masses $m_f(m_f)$ of $m_t = 170$ GeV, $m_b = 4.25$ GeV, $m_c = 1.27$ GeV.

where $x(\mu)$, $y(\mu)$, $\eta(\mu)$ defined by

$$x(\mu) = [\alpha_G/\alpha_1(\mu)]^{1/6}[\alpha_G/\alpha_2(\mu)]^{3/2} , \tag{19}$$

$$y(\mu) = \exp\left\{-\frac{1}{16\pi^2}\int_{\mu}^{M_G} \lambda_t^2(\mu')d\ln\mu'\right\} , \tag{20}$$

$$\eta(\mu) = \prod_{i=1,2,3} [\alpha_G/\alpha_i(\mu)]^{c_i/b_i} , \tag{21}$$

are to be evaluated at $\mu = m_t$ in Eq. (18). Henceforth x, y, η shall be understood as being evaluated at scale m_t when an argument is not explicitly specified. Typical values of these quantities obtained in Ref. [18] are $x = 1.52$, $y = 0.75 - 0.81$, $\eta = 10.3$ for a bottom-quark mass given by the Gasser-Leutwyler (GL) QCD sum rule determination $m_b = 4.25 \pm 0.1$ GeV [41] taken within its 90% confidence range and $\alpha_3 = 0.111$. The quantity y gives the scaling from M_G to m_t that arises from a heavy quark, beyond the scaling due to the gauge couplings. The factor $y(m_t)$ is constrained to lie in a narrow range of values by Eq. (18). The integral in Eq. (20) is crucial in explaining the m_b/m_τ ratio. In fact if λ_t is neglected then $y = 1$ and the m_b/m_τ ratio is found to be too large.

For a given value of m_t, there exist two solutions for $\tan\beta$. This fact can be understood qualitatively [42] by studying the one-loop RGE for $R_{b/\tau} \equiv \lambda_b/\lambda_\tau$:

$$\frac{dR_{b/\tau}}{dt} = \frac{R_{b/\tau}}{16\pi^2}\left(-\sum d_i g_i^2 + \lambda_t^2 + 3\lambda_b^2 - 3\lambda_\tau^2\right) . \tag{22}$$

For small $\tan\beta$ the bottom-quark and tau Yukawa couplings do not play a significant role in the RGE, and any particular value for m_b/m_τ is obtained for a unique value of $\lambda_t(m_t)$, which corresponds to a linear relationship between m_t and $\sin\beta$:

$$\frac{m_t}{\sin\beta} = \frac{v}{\sqrt{2}}\lambda_t(m_t) = \pi v\sqrt{\frac{2\eta}{3I}}\left[1 - y^{12}\right]^{1/2} , \tag{23}$$

where $v = 246$ GeV and

$$I = \int_{m_t}^{M_G} \eta(\mu')d\ln\mu' . \tag{24}$$

The numerical value for I from Ref. [18] is 113.79 for $m_t = 170$ GeV. For large $\tan\beta$, where the effects of λ_b and λ_τ on the running Yukawa couplings can be substantial, an increase in λ_b can be compensated in the RGE by a decrease in λ_t. Hence, for increasing $\tan\beta$, the correct prediction for m_b/m_τ is obtained for decreased values of the top-quark Yukawa coupling. Thus there is a second solution to the RGE for $R_{b/\tau}$ with a large value of $\tan\beta$. The inclusion of the two-loop effects does not alter these observations.

The one-loop RGE for $R_{s/\mu} \equiv \lambda_s/\lambda_\mu$,

$$\frac{dR_{s/\mu}}{dt} = \frac{R_{s/\mu}}{16\pi^2}\left(-\sum d_i g_i^2\right) , \tag{25}$$

is similar to Eq. (22), except that it receives no contribution from the dominant Yukawa couplings λ_t, λ_b, and λ_τ. When the value $R_{s/\mu}(M_G) = 1/3$ is assumed at the GUT scale, the prediction at the electroweak scale is

$$\frac{m_s}{m_\mu} = \frac{1}{3}\frac{\eta^{1/2}}{x}\frac{\eta_s}{\eta_\mu} . \tag{26}$$

Notice that this equation does not include the scaling parameter y because the top-quark Yukawa does not affect the running of the second-generation quarks and leptons. This relation for m_s/m_μ is in good agreement with the experimental values, but it is not as stringent as the m_b/m_τ relation due to the sizable uncertainty in the strange-quark mass. The result $m_s/m_\mu = 1.54$ was obtained in Ref. [18], to be compared with the GL determination [41] $m_s/m_\mu = 1.66 \pm 0.52$.

A popular strategy is to relate the mixing angles in the CKM matrix to ratios of quark masses, taking into account the evolution from the GUT scale in non-SUSY [43] or SUSY [44] models. For example, one popular GUT scale *Ansatz* is $|V_{cb}| \approx \sqrt{m_c/m_t}$ which requires a GUT boundary condition on $R_{c/t} \equiv \lambda_c/\lambda_t$ of

$$\sqrt{R_{c/t}(M_G)} = |V_{cb}(M_G)| . \tag{27}$$

The one-loop SUSY RGE for $R_{c/t}$ is

$$\frac{dR_{c/t}}{dt} = -\frac{R_{c/t}}{16\pi^2}[3\lambda_t^2 + \lambda_b^2] . \tag{28}$$

The corresponding one-loop SUSY RGE for the running CKM matrix element $|V_{cb}|$ is [44]

$$\frac{d|V_{cb}|}{dt} = -\frac{|V_{cb}|}{16\pi^2}[\lambda_t^2 + \lambda_b^2] . \tag{29}$$

The pure gauge coupling parts of the RGE's are not present in Eqs. (28) and (29) since $R_{c/t}$ and V_{cb} are ratios of elements from the up-quark Yukawa matrix and the down-quark Yukawa matrix.

Neglecting the nonleading effects of λ_b, the one-loop results of Ref. [6] at the electroweak scale obtained from evolution are

$$|V_{cb}(m_t)| = |V_{cb}(M_G)|y^{-1},$$
$$R_{c/t}(m_t) = R_{c/t}(M_G)y^{-3}, \tag{30}$$

or equivalently, using Eq. (27),

$$|V_{cb}(m_t)| = \sqrt{\frac{ym_c}{\eta_c m_t}}. \tag{31}$$

Since y is already well constrained by the b-mass relation of Eq. (18) [for the one-loop value of $\alpha_3(M_Z) = 0.111$], Eq. (31) requires that m_t must be large in order that $|V_{cb}|$ fall in the experimentally allowed range $0.032 - 0.054$ (and even then $|V_{cb}|$ is found to be at the upper limit of its allowed range). If, however, we use a larger value of $\alpha_3(M_Z)$ indicated by the two-loop equations, say 0.12, then η_c increases by about 14%, as shown in Fig. 3. Furthermore the increased values of the scaling parameters η and η_b require about a 9% decrease in y to explain the m_b/m_τ ratio in Eq. (18). The resulting $|V_{cb}|$ is reduced by about 12% and is then closer to its central experimental value. Of course, a consistent treatment at the two-loop level requires the two-loop generalization of Eq. (31) obtained by solving the full set of RGE's. One of the questions we will address subsequently is for what values of m_t and $\tan\beta$ can the $|V_{cb}|$ and the m_b/m_τ constraints be realized simultaneously [42].

The predictions above are all based upon the assumption that the couplings remain in the perturbative regime during the evolution from the GUT scale down to the electroweak scale. Otherwise it is not valid to use the RGE's, which are calculated order by order in perturbation theory. One can impose this perturbative unification condition as a constraint. For m_b at the lower end of the GL QCD sum-rule range $4.1 - 4.4$ GeV, the top-quark Yukawa coupling at the GUT scale, $\lambda_t(M_G)$, becomes large, as can be demonstrated from analytic solutions to the one-loop RGE's in the approximation that λ_b and λ_τ are neglected compared to λ_t (valid for small to moderate $\tan\beta$).

The top-quark Yukawa coupling at the GUT scale is given by

$$\lambda_t(M_G)^2 = \frac{4\pi^2}{3I}\left[\frac{1}{y^{12}} - 1\right]. \tag{32}$$

Taking [18] $\alpha_3(M_Z) = 0.111$ and $m_b = 4.25$ GeV and $m_t = 170$ GeV gives $\lambda_t(M_G) = 1.5$. Larger values of $\alpha_3(M_Z)$ lead to increased η_b via Eq. (11) giving smaller y in Eq. (18) and a correspondingly larger value of $\lambda_t(M_G)$. The quantity $\lambda_t(M_G)$ is plotted versus $\alpha_3(M_Z)$ in Fig. 4. Larger values of $\alpha_3(M_Z) \approx 0.12$ can yield $\lambda_t(M_G) \gtrsim 3$ that cast the perturbative unification in doubt. Keeping the gauge couplings fixed and varying m_b, one sees that smaller values of m_b also yield larger values of $\lambda_t(M_G)$.

The scaling parameter y is manifestly less than one by Eq. (20) since $\lambda_i^2 > 0$ in the region $m_t < \mu < M_G$. This implies an upper limit on m_b in Eq. (18) of

$$\frac{m_b}{m_\tau} \lesssim \frac{\eta^{1/2}}{x}\frac{\eta_b}{\eta_\tau}, \tag{33}$$

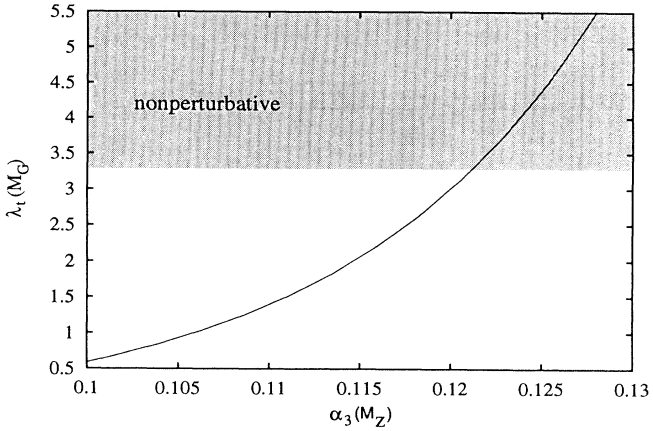

FIG. 4. The top-quark–Yukawa coupling at the GUT scale determined at the one-loop level is plotted versus $\alpha_3(M_Z)$ for $m_t = 170$ GeV and $m_b = 4.25$ GeV.

B. Two-loop numerical results

When the two-loop RGE's are considered, analytic solutions must be abandoned, but the same qualitative behavior is found in the numerical solutions. Furthermore, there is now the possibility that the bottom-quark Yukawa coupling at the GUT scale becomes nonperturbative for large values of $\tan\beta$. In our analysis we solve the two-loop RGE's of Eqs. (1)–(4) numerically [45], retaining all Yukawa couplings from the third generation.

First we choose a value of $\alpha_3(M_Z)$ that is consistent with experimental determinations and the preceding one-loop or two-loop evolution of the gauge couplings in the absence of Yukawa couplings. Specifically we take $\alpha_3(M_Z) = 0.11$ or $\alpha_3(M_Z) = 0.12$, to bracket the indicated $\alpha_3(M_Z)$ range. For each particular $\alpha_3(M_Z)$ we consider a range of values for $\tan\beta$ and $m_b(m_b)$. For each choice of $\alpha_3(M_Z)$, $\tan\beta$, m_b we choose an input value of m_t. The Yukawa couplings at scale m_t are then given by

$$\lambda_t(m_t) = \frac{\sqrt{2}m_t(m_t)}{v\sin\beta}, \quad \lambda_b(m_t) = \frac{\sqrt{2}m_b(m_b)}{\eta_b v\cos\beta},$$
$$\lambda_\tau(m_t) = \frac{\sqrt{2}m_\tau(m_\tau)}{\eta_\tau v\cos\beta}, \tag{34}$$

and the $\alpha_i(m_t)$ are determined by Eqs. (7) and (8) from the central values in Eq. (6) We take [11] $m_\tau = 1.784$ GeV. The running of the vacuum expectation value v between the fermion mass scales is negligible for the range of fermion masses considered here [5]. Starting at the scale m_t, we integrate the RGE's to the GUT scale, defined to be the scale at which $\alpha_1(\mu)$ and $\alpha_2(\mu)$ intersect. We then check to see if the equality $\lambda_b(M_G) = \lambda_\tau(M_G)$ holds to within 0.01%. If the b and τ Yukawa couplings satisfy this condition, the solution is accepted. If not, we choose another value of m_t and repeat the integration. Since our primary motivation here is to study the influ-

ence of the $\alpha_3(M_Z)$ value on the Yukawa couplings, we do not enforce the requirement that $\alpha_3(M_G)$ is equal to $\alpha_1(M_G)$ and $\alpha_2(M_G)$. Nevertheless the equality of α_1, α_2, and α_3 at M_G is typically violated by $\lesssim 4\%$ (2%) for $\alpha_3(M_Z) = 0.11$ (0.12). Such discrepancies could easily exist from threshold effects at the GUT scale [36, 37].

We also explore the effects of taking the SUSY scale above m_t. We proceed as described above, integrating the following two-loop standard model RGE's numerically from the top-quark mass to the SUSY scale:

$$\frac{dg_i}{dt} = \frac{g_i}{16\pi^2}\left[b_i^{\rm SM} g_i^2 + \frac{1}{16\pi^2}\left(\sum_{j=1}^{3} b_{ij}^{\rm SM} g_i^2 g_j^2 - \sum_{j=t,b,\tau} a_{ij}^{\rm SM} g_i^2 \lambda_j^2\right)\right], \tag{35}$$

$$\begin{aligned}\frac{d\lambda_t}{dt} = \frac{\lambda_t}{16\pi^2}\Bigg[&\Big[-\sum c_i^{\rm SM} g_i^2 + \frac{3}{2}\lambda_t^2 - \frac{3}{2}\lambda_b^2 + Y_2(S)\Big] \\ &+\frac{1}{16\pi^2}\Bigg(\frac{1187}{600}g_1^4 - \frac{23}{4}g_2^4 - 108 g_3^4 - \frac{9}{20}g_1^2 g_2^2 + \frac{19}{15}g_1^2 g_3^2 + 9 g_2^2 g_3^2 \\ &\quad + \left(\frac{223}{80}g_1^2 + \frac{135}{16}g_2^2 + 16 g_3^2\right)\lambda_t^2 - \left(\frac{43}{80}g_1^2 - \frac{9}{16}g_2^2 + 16 g_3^2\right)\lambda_b^2 \\ &\quad + \frac{5}{2}Y_4(S) - 2\lambda\left(3\lambda_t^2 + \lambda_b^2\right) + \frac{3}{2}\lambda_t^4 - \frac{5}{4}\lambda_t^2\lambda_b^2 + \frac{11}{4}\lambda_b^4 \\ &\quad + Y_2(S)\left(\frac{5}{4}\lambda_b^2 - \frac{9}{4}\lambda_t^2\right) - \chi_4(S) + \frac{3}{2}\lambda^2\Bigg)\Bigg],\end{aligned} \tag{36}$$

$$\begin{aligned}\frac{d\lambda_b}{dt} = \frac{\lambda_b}{16\pi^2}\Bigg[&\Big[-\sum c_i'^{\rm SM} g_i^2 + \frac{3}{2}\lambda_b^2 - \frac{3}{2}\lambda_t^2 + Y_2(S)\Big] \\ &+\frac{1}{16\pi^2}\Bigg(-\frac{127}{600}g_1^4 - \frac{23}{4}g_2^4 - 108 g_3^4 - \frac{27}{20}g_1^2 g_2^2 + \frac{31}{15}g_1^2 g_3^2 + 9 g_2^2 g_3^2 \\ &\quad - \left(\frac{79}{80}g_1^2 - \frac{9}{16}g_2^2 + 16 g_3^2\right)\lambda_t^2 + \left(\frac{187}{80}g_1^2 + \frac{135}{16}g_2^2 + 16 g_3^2\right)\lambda_b^2 \\ &\quad + \frac{5}{2}Y_4(S) - 2\lambda\left(\lambda_t^2 + 3\lambda_b^2\right) + \frac{3}{2}\lambda_b^4 - \frac{5}{4}\lambda_b^2\lambda_t^2 + \frac{11}{4}\lambda_t^4 \\ &\quad + Y_2(S)\left(\frac{5}{4}\lambda_t^2 - \frac{9}{4}\lambda_b^2\right) - \chi_4(S) + \frac{3}{2}\lambda^2\Bigg)\Bigg],\end{aligned} \tag{37}$$

$$\begin{aligned}\frac{d\lambda_\tau}{dt} = \frac{\lambda_\tau}{16\pi^2}\Bigg[&\Big[-\sum c_i''^{\rm SM} g_i^2 + \frac{3}{2}\lambda_\tau^2 + Y_2(S)\Big] \\ &+\frac{1}{16\pi^2}\Bigg(\frac{1371}{200}g_1^4 - \frac{23}{4}g_2^4 + \frac{27}{20}g_1^2 g_2^2 + \left(\frac{387}{80}g_1^2 + \frac{135}{16}g_2^2\right)\lambda_\tau^2 + \frac{5}{2}Y_4(S) - 6\lambda\lambda_\tau^2 \\ &\quad + \frac{3}{2}\lambda_\tau^4 - \frac{9}{4}Y_2(S)\lambda_\tau^2 - \chi_4(S) + \frac{3}{2}\lambda^2\Bigg)\Bigg],\end{aligned} \tag{38}$$

$$\begin{aligned}\frac{d\lambda}{dt} = \frac{1}{16\pi^2}\Bigg[&\left\{\frac{9}{4}\left(\frac{3}{25}g_1^4 + \frac{2}{5}g_1^2 g_2^2 + g_2^4\right) - \left(\frac{9}{5}g_1^2 + 9 g_2^2\right)\lambda + 4Y_2(S)\lambda - 4H(S) + 12\lambda^2\right\} \\ &+\frac{1}{16\pi^2}\Bigg(-78\lambda^3 + 18\left(\frac{3}{5}g_1^2 + 3 g_2^2\right)\lambda^2 + \left(-\frac{73}{8}g_2^4 + \frac{117}{20}g_1^2 g_2^2 + \frac{1887}{200}g_1^4\right)\lambda \\ &\quad + \frac{305}{8}g_2^6 - \frac{867}{120}g_1^2 g_2^4 - \frac{1677}{200}g_1^4 g_2^2 - \frac{3411}{1000}g_1^6 \\ &\quad - 64 g_3^2(\lambda_t^4 + \lambda_b^4) - \frac{8}{5}g_1^2(2\lambda_t^4 - \lambda_b^4 + 3\lambda_\tau^4) - \frac{3}{2}g_2^4 Y_2(S) + 10\lambda Y_4(S)\end{aligned}$$

$$+\frac{3}{5}g_1^2\left[\left(-\frac{57}{10}g_1^2+21g_2^2\right)\lambda_t^2+\left(\frac{3}{2}g_1^2+9g_2^2\right)\lambda_b^2+\left(-\frac{15}{2}g_1^2+11g_2^2\right)\lambda_\tau^2\right]$$
$$-24\lambda^2Y_2(S)-\lambda H(S)+6\lambda\lambda_t^2\lambda_b^2+20\left[3\lambda_t^6+3\lambda_b^6+\lambda_\tau^6\right]-12\left[\lambda_t^4\lambda_b^2+\lambda_t^2\lambda_b^4\right]\Bigg)\Bigg]\,. \tag{39}$$

Here

$$Y_2(S)=3\lambda_t^2+3\lambda_b^2+\lambda_\tau^2\,, \tag{40}$$

$$Y_4(S)=\frac{1}{3}\Bigg[3\sum c_i^{\rm SM}g_i^2\lambda_t^2+3\sum c_i'^{\rm SM}g_i^2\lambda_b^2+\sum c_i''^{\rm SM}g_i^2\lambda_\tau^2\Bigg]\,, \tag{41}$$

$$\chi_4(S)=\frac{9}{4}\left[3\lambda_t^4+3\lambda_b^4+\lambda_\tau^4-\frac{2}{3}\lambda_t^2\lambda_b^2\right]\,, \tag{42}$$

$$H(S)=3\lambda_t^4+3\lambda_b^4+\lambda_\tau^4\,, \tag{43}$$

and the coefficients $a^{\rm SM}$, $b^{\rm SM}$, and $c^{\rm SM}$ are given in the Appendix along with the full matrix structure.

The initial values for $\alpha_3(M_Z)$, m_b, and m_t are chosen as before; in addition we are required to specify the initial value of the quartic Higgs coupling λ at scale m_t. The Yukawa couplings at scale m_t are

$$\lambda_t(m_t)=\frac{\sqrt{2}m_t(m_t)}{v}\,,\quad \lambda_b(m_t)=\frac{\sqrt{2}m_b(m_b)}{\eta_b v}\,,$$
$$\lambda_t(m_t)=\frac{\sqrt{2}m_\tau(m_\tau)}{\eta_\tau v}\,, \tag{44}$$

and the $\alpha_i(m_t)$ are given by Eqs. (6)–(8). After integrating to the SUSY scale we require that the matching condition

$$\lambda(M_{\rm SUSY}^-)=\frac{1}{4}\left(\frac{3}{5}g_1^2(M_{\rm SUSY}^+)+g_2^2(M_{\rm SUSY}^+)\right)\cos^2 2\beta \tag{45}$$

is satisfied to within 0.1%. This condition [4, 33] results from integrating out the heavy Higgs doublet at $M_{\rm SUSY}$. Below this scale only a standard model Higgs boson remains with its quartic coupling given by Eq. (45). We also apply the matching conditions

$$g_i(M_{\rm SUSY}^-)=g_i(M_{\rm SUSY}^+)\,, \tag{46}$$
$$\lambda_t(M_{\rm SUSY}^-)=\lambda_t(M_{\rm SUSY}^+)\sin\beta\,, \tag{47}$$
$$\lambda_b(M_{\rm SUSY}^-)=\lambda_b(M_{\rm SUSY}^+)\cos\beta\,, \tag{48}$$
$$\lambda_\tau(M_{\rm SUSY}^-)=\lambda_\tau(M_{\rm SUSY}^+)\cos\beta\,. \tag{49}$$

If Eq. (45) is not satisfied we choose another input value of $\lambda(m_t)$ and repeat the process. We allow $\tan\beta$ to span a wide grid of values. After obtaining a satisfactory value of λ that meets the boundary condition above, we integrate the two-loop SUSY RGE's to the GUT scale, defined by the equality $\alpha_1(M_G)=\alpha_2(M_G)$. At the GUT scale we require $\lambda_b(M_G)=\lambda_\tau(M_G)$ to within 0.1%. If this condition is not met, we repeat the entire process, choosing other initial values for m_t and λ.

The parameter β also runs in going from the SUSY scale to the electroweak scale [33]. However, this effect is small and we neglect it here.

In Fig. 5 the resulting contours of constant m_b are given in the m_t-$\tan\beta$ plane [4, 17] for the choices of $\alpha_3(M_Z)=0.11$ and 0.12 and the supersymmetry scales $M_{\rm SUSY}=m_t$ and 1 TeV. The contours shown are $m_b=4.1, 4.25, 4.4$ GeV (corresponding to the central value of m_b and its 90% confidence range from the GL QCD sum-rule determination) and $m_b=5.0$ GeV (representing a typical constituent b-quark mass value; this latter contour is included only for comparison with other work). For a given m_b and $m_t \lesssim 175$ GeV, there is a high solution and a low solution for $\tan\beta$ as anticipated in Sec. III A. Thus, once m_t is experimentally known and the choice of m_b resolved by other considerations (such as the CKM matrix elements addressed subsequently), the assumption of Yukawa unification at the GUT scale will select two possible values for $\tan\beta$. For example, for $m_t=150$ GeV and $m_b=4.25$ GeV, the solutions with $\alpha_3(M_Z)=0.11$ are

$$\tan\beta=1.35 \quad \text{or} \quad \tan\beta=56\,. \tag{50}$$

For $m_t \lesssim 175$ GeV the low solution is well approximated by

$$\sin\beta=0.78\left(\frac{m_t}{150\ \text{GeV}}\right)\,. \tag{51}$$

Such knowledge of $\tan\beta$ would greatly simplify SUSY Higgs analyses [46]. Without imposing any other constraints, the top-quark mass m_t can be arbitrarily small.

The plots rise very steeply for the maximal value of m_t. This results because the linear relation exhibited in Eq. (23) and in the plot in Ref. [18] between m_t and $\sin\beta$ is mapped into a vertical line for sufficiently large $\tan\beta$ ($\gtrsim 10$). The deviation of these contours from being strictly vertical results from the contributions of λ_b and λ_τ to the Yukawa coupling evolution.

An upper limit on m_t is determined entirely by the

TABLE III. Maximum values of $m_t(m_t)$ in GeV consistent with the 90% confidence levels of the $m_b(m_b)$ values of GL.

$M_{\rm SUSY}$ \ $\alpha_3(M_Z)$	0.11	0.12
m_t	187	193
1 TeV	192	199

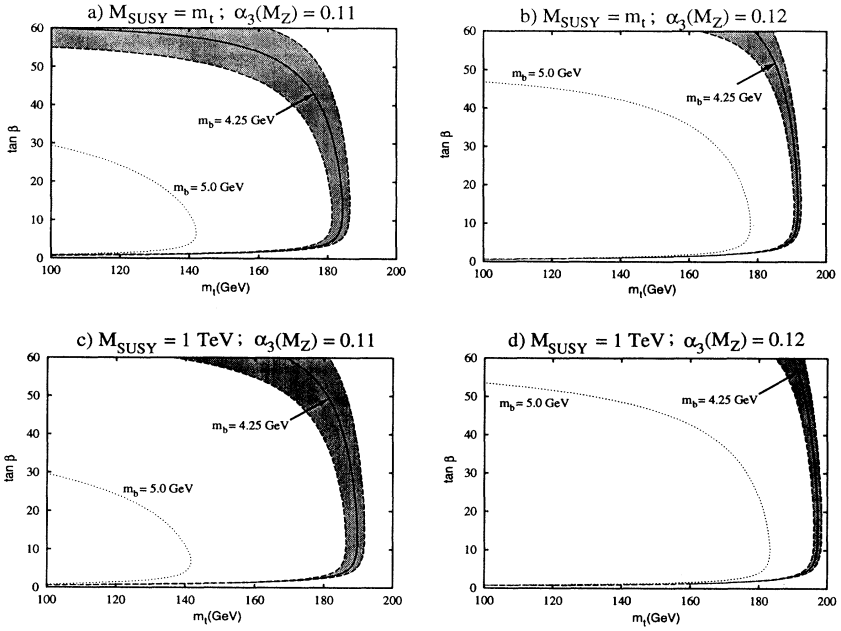

FIG. 5. Contours of constant m_b in the m_t-tanβ plane obtained from the RGE's with (a) $M_{\rm SUSY} = m_t$, $\alpha_3(M_Z) = 0.11$; (b) $M_{\rm SUSY} = m_t$, $\alpha_3(M_Z) = 0.12$; (c) $M_{\rm SUSY} = 1$ TeV, $\alpha_3(M_Z) = 0.11$; (d) $M_{\rm SUSY} = 1$ TeV, $\alpha_3(M_Z) = 0.12$. The shaded band corresponds to the 90% confidence level range of m_b from Ref. [41] ($m_b = 4.1$–4.4 GeV); the dotted curve corresponds to $m_b = 5.0$ GeV. The curves shift to higher m_t values for increasing $\alpha_3(M_Z)$ or increasing $M_{\rm SUSY}$.

m_b/m_τ ratio. We find the m_t upper limits shown in Table III for the two choices of $\alpha_3(M_Z)$. It is interesting that the predicted upper limit for m_t coincides with that allowed by electroweak radiative corrections [11].

Our contours of m_b/m_τ in Fig. 5 have about a 10% higher m_b than those given in Ref. [17] presumably because they employed the one-loop QCD results for the scaling factors η_f with the two-loop expression for α_3 rather than the three-loop QCD for both η_f and α_3 that we use here.

As $\alpha_3(M_Z)$ gets larger, smaller values of y are needed to obtain the correct m_b/m_τ ratio. In turn larger values of $\lambda_t(\mu)$ are needed via Eq. (20). For $\alpha_3(M_Z) \gtrsim 0.12$ and $m_b \lesssim 4.2$ GeV, the value of $\lambda_t(\mu)$ near the GUT scale can be driven into the nonperturbative regime. In Fig. 6 we show the values of $\lambda_t(M_G)$ and $\lambda_b(M_G)$ obtained for the solutions in Fig. 5. Fixed points in the quark Yukawa couplings exist at $\lambda \approx 1$, so a Yukawa coupling only slightly larger than the fixed point at the scale m_t can diverge as it is evolved to the GUT scale. For large values of the Yukawa couplings the two-loop contributions to the RGE's contribute a fraction x of the one-loop contributions when

$$\lambda_t = \sqrt{\frac{6(16\pi^2 x)}{22}} \approx 6.5\sqrt{x}\,, \tag{52}$$

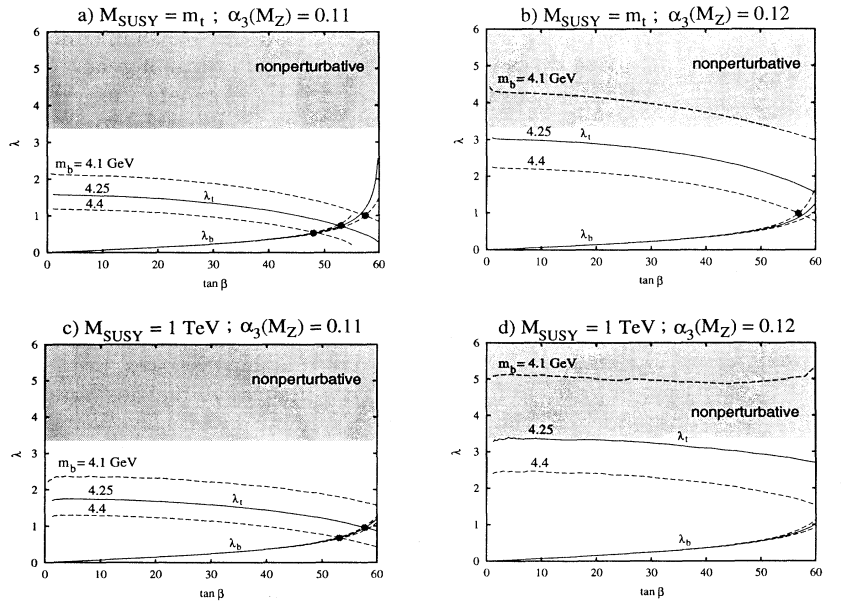

FIG. 6. The Yukawa couplings $\lambda_t(M_G)$ and $\lambda_b(M_G) = \lambda_\tau(M_G)$ at the GUT scale with (a) $M_{\rm SUSY} = m_t$, $\alpha_3(M_Z) = 0.11$; (b) $M_{\rm SUSY} = m_t$, $\alpha_3(M_Z) = 0.12$; (c) $M_{\rm SUSY} = 1$ TeV, $\alpha_3(M_Z) = 0.11$; (d) $M_{\rm SUSY} = 1$ TeV, $\alpha_3(M_Z) = 0.12$. The Yukawa couplings become larger for higher $\alpha_3(M_Z)$ or higher $M_{\rm SUSY}$. The perturbative condition $\lambda \lesssim 3.3$ from Eq. (52) is satisfied except for the lowest b mass value $m_b = 4.1$ GeV for $\alpha_3(M_Z) = 0.12$. The solid dots denote $\lambda_\tau = \lambda_b = \lambda_t$ unification.

$$\lambda_b = \sqrt{\frac{7(16\pi^2 x)}{28}} \approx 6.3\sqrt{x}\,, \tag{53}$$

as can be deduced from Eqs. (2) and (3). When $x \approx 1$ we are clearly in the nonperturbative regime. If we adopt the criteria that the two-loop effects always be less than a quarter of the one-loop effects, then λ_t and λ_b are nonperturbative when they remain below 3.3 and 3.1 respectively all the way to the GUT scale. This is true for all of the curves presented in Fig. 6, except for the $m_b = 4.1$ GeV contours for $\alpha_3(M_Z) = 0.12$; hence the exact position of this contour cannot be predicted with accuracy.

In Fig. 7 we show the evolution of the Yukawa couplings from the SUSY scale to the GUT scale. The nonperturbative regime for the case discussed above occurs only near the GUT scale.

In some SO(10) GUT models the top-quark Yukawa coupling λ_t is unified with the λ_b and λ_τ at the GUT scale. Imposing this constraint selects a unique value for $\tan\beta$ and m_t [17, 47]. This solution is given by the intersection of $\lambda_t(M_G)$ and $\lambda_b(M_G)$, which occurs for large $\tan\beta \gtrsim 50$: see Fig. 6.

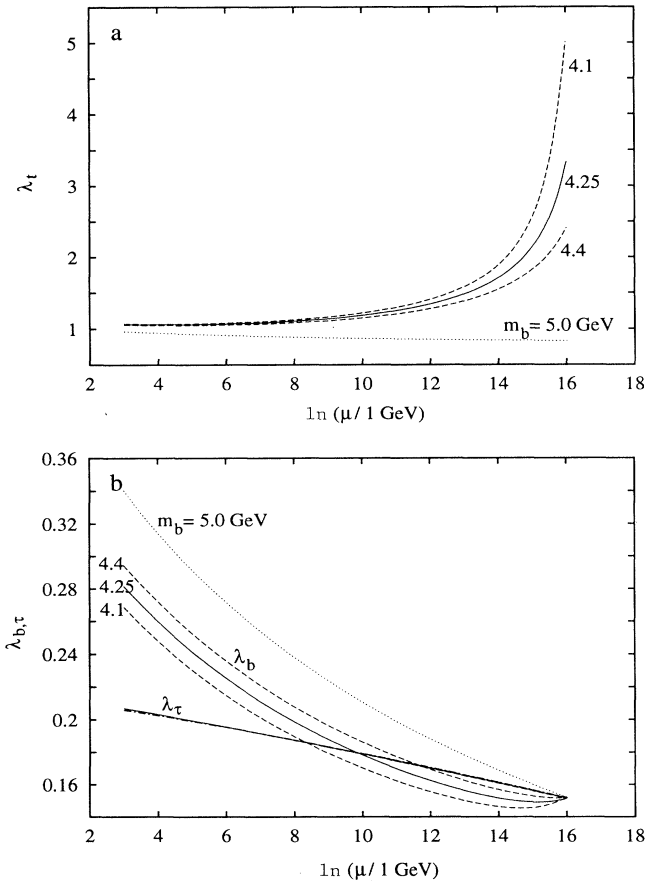

FIG. 7. Two-loop evolution of the Yukawa couplings (a) $\lambda_t(\mu)$, (b) $\lambda_b(\mu)$, $\lambda_\tau(\mu)$ from low energies to the GUT scale for the case $\alpha_3(M_Z) = 0.12$ and $M_{\rm SUSY} = 1$ TeV. We take $\tan\beta = 20$ and the values of $m_t = 198$, 197, 196, 181 GeV specified by the $m_b = 4.1$, 4.25, 4.4, 5.0 GeV contours in Fig. 5(d).

One could also consider the unification of the Yukawa couplings at some scale other than that at which the gauge couplings unify [4, 17]. Since $R_{b/\tau}$ increases as it evolves from the GUT scale to the electroweak scale, Yukawa unification at a scale larger than the gauge coupling unification scale gives a larger m_b/m_τ ratio.

The authors of Ref. [4] predict the light physical Higgs-boson mass rather precisely. However, this prediction is related to their assumption (and the one we use here) that the heavy Higgs doublet is integrated out at $M_{\rm SUSY}$. This means that the heavy physical Higgs bosons have masses $M_H \approx M_A \approx M_{H^\pm} \approx M_{\rm SUSY} \gg M_Z$, which requires that the light Higgs-boson mass is close to its upper limit. The relation of $\sin\beta$ to m_t then fixes the one-loop corrections to the light Higgs-boson mass.

IV. FERMION MASS *ANSATZ*

By assuming an *Ansatz* for Yukawa matrices at the GUT scale and evolving these matrices down to the electroweak scale, predictions can be obtained for the quark and lepton masses and the CKM matrix elements [4, 6, 7, 16]. Much work has been done on individual relations such as $|V_{ud}| \approx \sqrt{m_s/m_d}$ and $|V_{cb}| \approx \sqrt{m_c/m_t}$ which are imposed at the GUT scale as described in Sec. III. Recently interest has been revived in models that involve several such relations, leading to a number of predictions for quark masses and CKM matrix elements at the electroweak scale [4, 6–8]. The relations evolve according to RGE's, and the main effects are determined by the largest couplings. For moderate values of $\tan\beta$ (i.e., $\tan\beta \lesssim 10$), these are the gauge couplings g_i and the top-quark Yukawa coupling λ_t. For large values of $\tan\beta (\approx m_t/m_b)$ the effects of λ_b and λ_τ can also be significant. Various individual relations at the GUT scale such as $|V_{cb}| \approx \sqrt{m_c/m_t}$ can be satisfied for certain choices of these Yukawa couplings. The remarkable aspect of these fermion mass *Ansätze* is that many relations can be made to work at one time. We shall concentrate in this section on two predictive ways of generating mixing between the second and third generations which put those mixing contributions entirely in the up-quark Yukawa matrix [4, 6, 16] (the **U** Model) or entirely in the down-quark Yukawa matrix [7] (the **D** Model).

A. The U Model

Relations between fermion masses and CKM matrix elements date back at least to 1968 [19], when the Cabibbo angle was related to the quark masses, $\tan\theta_C = \sqrt{m_d/m_s}$. Subsequently these flavor symmetries were extended to the general two generation case by Weinberg and Wilczek and Zee [20] and to three generations by Fritzsch [21]. Georgi and Jarlskog [22] then postulated that such mass matrix *Ansätze* are valid at the GUT scale, and determined the zero structure in an SU(5) theory, obtaining an asymmetric charge $-1/3$ mass matrix **D**. Georgi and Nanopoulos [23] then modified this

Ansatz by going to an SO(10) model, obtaining a symmetric form for **D**. Harvey, Ramond, and Reiss [16] realized the Georgi-Jarlskog-Nanopoulos form in an SO(10) GUT theory with specific Higgs representations, namely a (complex) **10** and three **126** multiplets. When all but one of the arbitrary phases in the GUT matrices are rotated away, the Yukawa matrices at the GUT scale have the form [6]

$$\mathbf{U}=\begin{pmatrix}0 & C & 0\\ C & 0 & B\\ 0 & B & A\end{pmatrix},\qquad \mathbf{D}=\begin{pmatrix}0 & Fe^{i\phi} & 0\\ Fe^{-i\phi} & E & 0\\ 0 & 0 & D\end{pmatrix}, \tag{54}$$

$$\mathbf{E}=\begin{pmatrix}0 & F & 0\\ F & -3E & 0\\ 0 & 0 & D\end{pmatrix}. \tag{55}$$

In a recent landmark paper [6] Dimopoulos, Hall, and Raby considered the supersymmetric evolution of this GUT texture down to low energies and showed that the resulting predictions are in accord with the experimental data on quark and lepton masses and CKM elements.

Renormalization-group evolution generates nonzero entries in the above Yukawa matrices and also splits $B_1 \equiv \mathbf{U}_{23}$ and $B_2 \equiv \mathbf{U}_{32}$ to give the matrices at the electroweak scale of the form

$$\mathbf{U}=\begin{pmatrix}0 & C & 0\\ C & \delta_u & B_1\\ 0 & B_2 & A\end{pmatrix},\qquad \mathbf{D}=\begin{pmatrix}0 & Fe^{i\phi} & 0\\ Fe^{-i\phi} & E & \delta_d\\ 0 & 0 & D\end{pmatrix}, \tag{56}$$

$$\mathbf{E}=\begin{pmatrix}0 & F' & 0\\ F' & -3E' & 0\\ 0 & 0 & D'\end{pmatrix}. \tag{57}$$

The quantities A, D, and D' are equivalent to λ_t, λ_b, and λ_τ respectively up to subleading corrections in the mass matrix diagonalization. The one-loop solutions [6] to leading order in the hierarchy can be obtained analytically neglecting λ_b and λ_τ. The one-loop results for the CKM elements at the scale m_t are

$$|V_{us}|=\left[\frac{\eta_s m_d}{\eta_d m_s}+\frac{\eta_c m_u}{\eta_u m_c}+2\sqrt{\frac{\eta_s\eta_c m_u m_d}{\eta_d\eta_u m_s m_c}}\cos\phi\right]^{1/2}, \tag{58}$$

$$|V_{cb}|=\sqrt{\frac{y m_c}{\eta_c m_t}}, \tag{59}$$

$$\left|\frac{V_{ub}}{V_{cb}}\right|=\sqrt{\frac{\eta_c m_u}{\eta_u m_c}}, \tag{60}$$

where $\eta_i(m_t)$ is defined by Eq. (11) and $y(m_t)$ by Eq. (20). The angle ϕ is *a priori* arbitrary. The down-type quark masses are related to the corresponding lepton masses by

$$m_d=\frac{\eta^{1/2}}{x}\frac{\eta_d}{\eta_e}3m_e, \tag{61}$$

$$m_s=\frac{\eta^{1/2}}{x}\frac{\eta_s}{\eta_\mu}\frac{m_\mu}{3}, \tag{62}$$

$$m_b=y\frac{\eta^{1/2}}{x}\frac{\eta_b}{\eta_\tau}m_\tau. \tag{63}$$

Using the general expressions for the two-loop RGE's given in the Appendix and keeping only terms unsuppressed by the hierarchy, one obtains Eqs. (1)–(4) as well as

$$\frac{dB_1}{dt}=\frac{B_1}{16\pi^2}\left[\left(-\sum c_i g_i^2+6\lambda_t^2+\frac{\lambda_t\lambda_b\delta_d}{B_1}\right)+\frac{1}{16\pi^2}\left(\sum\left(c_i b_i+c_i^2/2\right)g_i^4+g_1^2g_2^2+\frac{136}{45}g_1^2g_3^2+8g_2^2g_3^2+\lambda_t^2\left(\frac{6}{5}g_1^2+6g_2^2+16g_3^2\right)+\frac{2}{5}\frac{\lambda_t\lambda_b\delta_d}{B_1}g_1^2-\left\{22\lambda_t^4+5\lambda_t^2\lambda_b^2+\frac{\lambda_t\lambda_b\delta_d}{B_1}\left(5\lambda_b^2+\lambda_\tau^2\right)\right\}\right)\right], \tag{64}$$

$$\frac{dB_2}{dt}=\frac{B_2}{16\pi^2}\left[\left(-\sum c_i g_i^2+6\lambda_t^2+\lambda_b^2\right)+\frac{1}{16\pi^2}\left(\sum\left(c_i b_i+c_i^2/2\right)g_i^4+g_1^2g_2^2+\frac{136}{45}g_1^2g_3^2+8g_2^2g_3^2+\lambda_t^2\left(\frac{6}{5}g_1^2+6g_2^2+16g_3^2\right)+\frac{2}{5}\lambda_b^2g_1^2-\left\{22\lambda_t^4+5\lambda_t^2\lambda_b^2+5\lambda_b^4+\lambda_b^2\lambda_\tau^2\right\}\right)\right], \tag{65}$$

$$\frac{d\delta_u}{dt} = \frac{\delta_u}{16\pi^2}\left[\left(-\sum c_i g_i^2 + 3\lambda_t^2 + 3\frac{\lambda_t B_1 B_2}{\delta_u} + \frac{\lambda_b \delta_d B_2}{\delta_u}\right)\right.$$
$$+\frac{1}{16\pi^2}\left(\sum\left(c_i b_i + c_i^2/2\right) g_i^4 + g_1^2 g_2^2 + \frac{136}{45} g_1^2 g_3^2 + 8 g_2^2 g_3^2\right.$$
$$+\lambda_t^2\left(\frac{4}{5}g_1^2 + 16 g_3^2\right) + \frac{\lambda_t B_1 B_2}{\delta_u}\left(\frac{2}{5}g_1^2 + 6 g_2^2\right) + \frac{2}{5}\frac{\lambda_b \delta_d B_2}{\delta_u} g_1^2$$
$$\left.\left.\left. - \left\{9\lambda_t^4 + 3\lambda_t^2\lambda_b^2 + \frac{\lambda_t B_1 B_2}{\delta_u}\left(13\lambda_t^2 + 2\lambda_b^2\right) + \frac{\lambda_b \delta_d B_2}{\delta_u}\left(5\lambda_b^2 + \lambda_\tau^2\right)\right\}\right)\right], \tag{66}$$

$$\frac{d\delta_d}{dt} = \frac{\delta_d}{16\pi^2}\left[\left(-\sum c_i' g_i^2 + 6\lambda_b^2 + \lambda_\tau^2 + \frac{\lambda_t \lambda_b B_1}{\delta_d}\right)\right.$$
$$+\frac{1}{16\pi^2}\left(\sum\left(c_i' b_i + c_i'^2/2\right) g_i^4 + g_1^2 g_2^2 + \frac{8}{9} g_1^2 g_3^2 + 8 g_2^2 g_3^2\right.$$
$$+\lambda_b^2\left(\frac{2}{5}g_1^2 + 6 g_2^2 + 16 g_3^2\right) + \frac{6}{5}\lambda_\tau^2 g_1^2 + \frac{4}{5}\frac{\lambda_t \lambda_b B_1}{\delta_d} g_1^2$$
$$\left.\left.\left. - \left\{22\lambda_b^4 + 5\lambda_t^2\lambda_b^2 + 3\lambda_b^2\lambda_\tau^2 + 3\lambda_\tau^4 + \frac{\lambda_t \lambda_b B_1}{\delta_d} 5\lambda_t^2\right\}\right)\right]. \tag{67}$$

Notice that since $(1/B_2)dB_2/dt = (1/\lambda_t)d\lambda_t/dt$, the ratio B_2/λ_t is constant over all scales and is in particular equal to its value at the GUT scale $B_2(M_G)/\lambda_t(M_G)$.

With these RGE's we can include the additional experimental constraints from the charm-quark mass m_c and the CKM matrix element $|V_{cb}|$ to determine the allowed region of the **U** model in the m_t-$\tan\beta$ plane. An analysis at the one-loop level neglecting λ_b and λ_τ relative to λ_t was presented in Ref. [18].

The Yukawa matrices are diagonalized by unitary matrices $V_u^L, V_u^R, V_d^L, V_d^R$ so that $\mathbf{U}^{\rm diag} = V_u^L \mathbf{U} V_u^{R\dagger}$ and $\mathbf{D}^{\rm diag} = V_d^L \mathbf{D} V_d^{R\dagger}$. The CKM matrix is then given by $V_{\rm CKM} = V_u^L V_d^{L\dagger}$. We define a "running" CKM matrix by diagonalizing the Yukawa matrices **U** and **D** at any scale t. We find that λ_c/λ_t and $|V_{cb}|$ are described in terms of the Yukawa matrices by

$$R_{c/t} \equiv \frac{\lambda_c}{\lambda_t} = \left(\frac{B_1 B_2}{\lambda_t^2} - \frac{\delta_u}{\lambda_t}\right), \tag{68}$$

$$|V_{cb}| = \frac{B_1}{\lambda_t} - \frac{\delta_d}{\lambda_b}, \tag{69}$$

with

$$\frac{m_c}{m_t} = \eta_c R_{c/t}(m_t). \tag{70}$$

To leading order in the mass hierarchy, the ratio $R_{c/t}$ is given by the ratio of eigenvalues of the 2×2 submatrix of **U** in the second and third generations while V_{cb} is given by the difference in the rotation angles needed to rotate away the upper-right-hand entry in the submatrices of **U** and **D**. Given that the mass hierarchies exist, there is a simple iterative numerical procedure for diagonalizing the mass matrices **U** and **D** and obtaining the CKM matrix. We have checked that the corrections to the above formulas from contributions subleading in the mass hierarchy are small.

It is straightforward to derive the resulting renormalization-group equations from Eqs. (64)–(67):

$$\frac{dR_{c/t}}{dt} = -\frac{R_{c/t}}{16\pi^2}\left(\left(3\lambda_t^2 + \lambda_b^2\right) + \frac{1}{16\pi^2}\left[\lambda_t^2\left(\frac{2}{5}g_1^2 + 6 g_2^2\right) + \frac{2}{5}\lambda_b^2 g_1^2 - \left(13\lambda_t^4 + 2\lambda_t^2\lambda_b^2 + 5\lambda_b^4 + \lambda_b^2\lambda_\tau^2\right)\right]\right), \tag{71}$$

$$\frac{d|V_{cb}|}{dt} = -\frac{|V_{cb}|}{16\pi^2}\left[\left(\lambda_t^2 + \lambda_b^2\right) + \frac{1}{16\pi^2}\left(\frac{4}{5}\lambda_t^2 g_1^2 + \frac{2}{5}\lambda_b^2 g_1^2 - \left(5\lambda_t^4 + 5\lambda_b^4 + \lambda_b^2\lambda_\tau^2\right)\right)\right], \tag{72}$$

The corresponding evolution equations in the standard model are given by

$$\frac{dR_{c/t}}{dt} = -\frac{R_{c/t}}{16\pi^2}\left[\left(\frac{3}{2}\lambda_t^2 - \frac{3}{2}\lambda_b^2\right) + \frac{1}{16\pi^2}\left(\lambda_t^2\left(\frac{223}{80}g_1^2 + \frac{135}{16}g_2^2 + 16 g_3^2\right) - \lambda_b^2\left(\frac{43}{80}g_1^2 - \frac{9}{16}g_2^2 + 16 g_3^2\right)\right.\right.$$
$$\left.\left. -2\lambda(3\lambda_t^2 + \lambda_b^2) - \left(\frac{21}{4}\lambda_t^4 + \frac{17}{4}\lambda_t^2\lambda_b^2 - \frac{13}{2}\lambda_b^4 + \frac{9}{4}\lambda_t^2\lambda_\tau^2 - \frac{5}{4}\lambda_b^2\lambda_\tau^2\right)\right)\right], \tag{73}$$

$$\frac{d|V_{cb}|}{dt} = \frac{|V_{cb}|}{16\pi^2}\left[\left(\frac{3}{2}\lambda_t^2+\frac{3}{2}\lambda_b^2\right)+\frac{1}{16\pi^2}\left(\lambda_t^2\left(\frac{79}{80}g_1^2-\frac{9}{16}g_2^2+16g_3^2\right)+\lambda_b^2\left(\frac{43}{80}g_1^2-\frac{9}{16}g_2^2+16g_3^2\right)\right.\right.$$
$$\left.\left.+2\lambda(\lambda_t^2+\lambda_b^2)-\left(\frac{13}{2}\lambda_t^4+\frac{11}{2}\lambda_t^2\lambda_b^2+\frac{13}{2}\lambda_b^4+\frac{5}{4}\lambda_t^2\lambda_\tau^2+\frac{5}{4}\lambda_b^2\lambda_\tau^2\right)\right)\right]. \quad (74)$$

The evolution equations in Eqs. (73) and (74) are obtained from the two-loop RGE's of the standard model given in Ref. [28] and in the Appendix.

In the supersymmetric model $|V_{cb}|$ increases with the running from the GUT scale to the electroweak scale [44]; this is evident at the two-loop level in Eq. (72). The opposite behavior occurs in Eq. (74) for the nonsupersymmetric standard model where $|V_{cb}|$ decreases as the running mass decreases [43]. Figure 8 shows the running of $|V_{cb}|$ for the cases $M_{\rm SUSY} = m_t$ and 1 TeV. In contrast to $|V_{cb}|$ the ratio $R_{c/t}$ increases monotonically as the running mass decreases in both the standard model and supersymmetric model cases.

We stress that Eqs. (71)–(74) are the correct evolution equations regardless of the fermion mass *Ansatz* at the GUT scale. Changing the *Ansatz* just changes the boundary conditions at the GUT scale (terms subleading in the mass hierarchy differ between models, but this is a negligible effect). In a model for which the relationship $|V_{cb}| = \sqrt{\lambda_c/\lambda_t}$ holds (as in the **U** model), this boundary condition is $\sqrt{R_{c/t}(M_G)} = |V_{cb}(M_G)|$. In the **D** model, to be described below, the mixing between the second and third generations arises in the down-quark Yukawa matrix alone, and so in his model $R_{c/t}$ and $|V_{cb}|$ are unrelated at the GUT scale.

In our analysis of the CKM constraints we proceed as in the discussion of the calculation for Fig. 5. We numerically solve the two-loop RGE's as given by Eqs. (1)–(4), (71), and (72) for the case $M_{\rm SUSY} = m_t$. As before, we consider the representative choices $\alpha_3(M_Z) = 0.11$ and $\alpha_3(M_Z) = 0.12$. For each $\alpha_3(M_Z)$ choice, we consider a grid of $\tan\beta$ values, holding $|V_{cb}(m_t)|$ and m_c fixed. We then choose input values for m_t and m_b [given $\alpha_3(M_Z)$, $\tan\beta$, $|V_{cb}|$, m_c] in terms of which all running parameters are uniquely specified at m_t: $\lambda_t(m_t)$, $\lambda_b(m_t)$, and $\lambda_\tau(m_t)$ are given by Eq. (34), $\alpha_i(m_t)$ are determined by Eqs. (7) and (8) using the central values in Eq. (6), $R_{c/t}$ is given by Eq. (70), and $|V_{cb}|$ at scale m_t is an input. After integrating the RGE's from m_t to M_G we check the constraints

$$\lambda_b(M_G) = \lambda_\tau(M_G)\,, \quad (75a)$$
$$\sqrt{R_{c/t}(M_G)} = |V_{cb}(M_G)|\,. \quad (75b)$$

If either of these conditions is not satisfied to within 0.2%, we choose another input value for m_t and m_b and repeat the integration.

We also carry out the RGE calculations with a SUSY scale at 1 TeV. This is done exactly as described in the previous section. In addition to the other parameters, we choose an input value for the quartic Higgs coupling λ at scale m_t. We then integrate the two-loop standard model RGE's to the SUSY scale and require that Eq. (45) hold to within 0.1%. For such solutions we apply the other appropriate boundary conditions [given by Eqs. (46)–(49)] and integrate the two-loop SUSY RGE's to the GUT scale, where we require that $\lambda_b(M_G) = \lambda_\tau(M_G)$ and $\sqrt{R_{c/t}(M_G)} = |V_{cb}(M_G)|$ to within 0.2%. In our calculation we require that m_b, m_c, and $|V_{cb}|$ be within the experimentally determined 90% confidence levels of the quark mass determinations of GL ($4.1 < m_b < 4.4$ GeV, $1.19 < m_c < 1.35$ GeV) and the recent Particle Data Group value [11] for $|V_{cb}|$ ($0.032 < |V_{cb}| < 0.054$).

In Fig. 9 the contours of constant $|V_{cb}|$ are shown in the

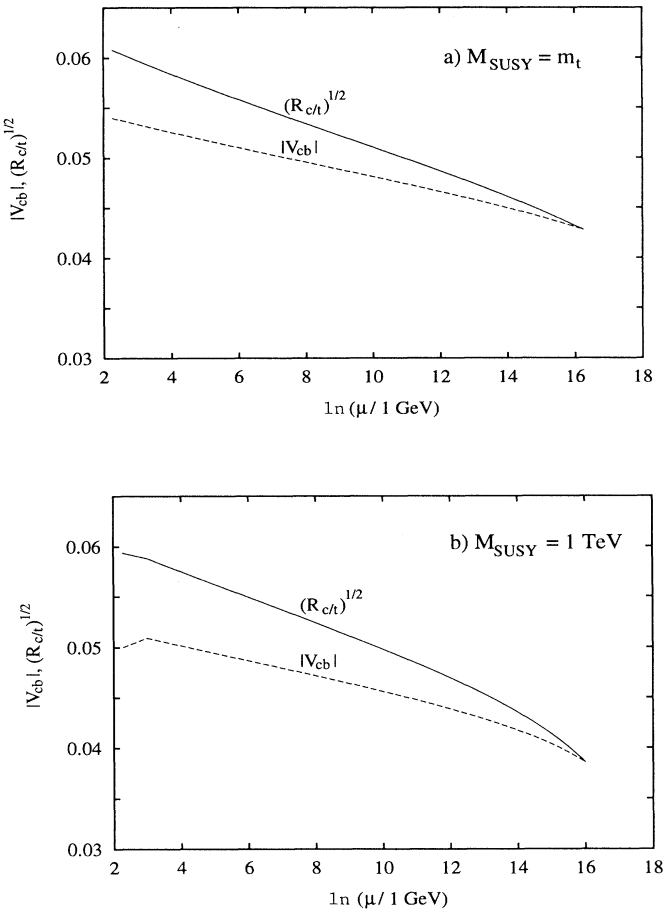

FIG. 8. Two-loop evolution of the quark Yukawa ratio $R_{c/t} \equiv \lambda_c/\lambda_t$ and the CKM matrix element $|V_{cb}|$ for (a) $M_{\rm SUSY} = m_t$ and (b) $M_{\rm SUSY} = 1$ TeV. We have taken $\alpha_3 = 0.11$, $\tan\beta = 5$ and have chosen the top- and bottom-quark masses such that $\sqrt{R_{c/t}(M_G)} = |V_{cb}(M_G)|$ and $m_c = 1.27$ GeV: (a) $|V_{cb}(m_t)| = 0.054$, $m_t = 180$ GeV, $m_b = 4.33$ GeV; (b) $|V_{cb}(m_t)| = 0.050$, $m_t = 189$ GeV, $m_b = 4.14$ GeV.

m_t-$\tan\beta$ plane for a fixed $m_c = 1.27$ GeV. In Figs. 10 and 11 we show the contours obtained by applying only the constraint in Eq. (75a) as in Fig. 5 along with the contours obtained by applying both Eqs. (75a) and (75b) for fixed m_c as in Fig. 9. In Fig. 10 the value of m_c is fixed at 1.27 GeV and contours of $|V_{cb}|$ are shown. In Fig. 11 $|V_{cb}|$ is fixed at its maximum allowed experimental value of $|V_{cb}| = 0.054$ (at 90% C.L.) and three values of m_c are plotted (corresponding to the central m_c value and the 90% C.L. values from GL).

For large $\tan\beta$ the effects of including λ_b and λ_τ in the RGE's increase $|V_{cb}|$. In order to satisfy $|V_{cb}| < 0.054$, the maximum allowed value of $\tan\beta$ for $\alpha_3(M_Z) = 0.11$ is about 50(60) for $M_{\rm SUSY} = m_t(1\ {\rm TeV})$; see Fig. 11. For this value of $\alpha_3(M_Z)$ the **U** model predicts that $|V_{cb}|$ still lies at the upper end of its allowed 90% confidence level range when the effects of λ_b and λ_τ at large $\tan\beta$ are included in the two-loop RGE's; see Fig. 10. Allowing m_b to become larger than the narrow window $m_b = 4.1 - 4.4$ GeV requires bigger $|V_{cb}|$, which is unacceptable. The higher b mass contour $m_b = 5$ GeV is not consistent with

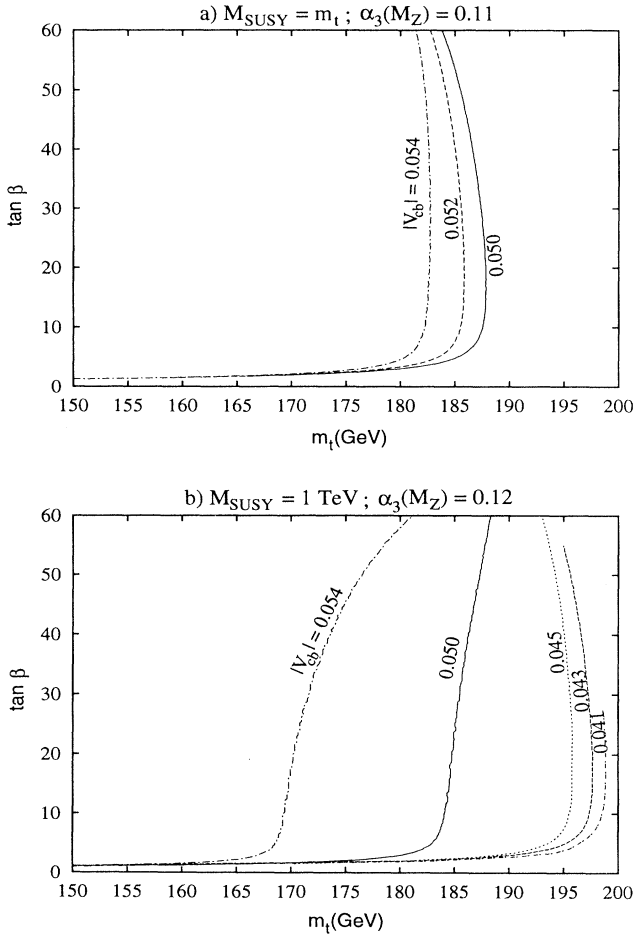

FIG. 9. Contours for constant $|V_{cb}|$ at fixed $m_c = 1.27$ GeV in the m_t-$\tan\beta$ plane obtained from the RGE's with (a) $M_{\rm SUSY} = m_t$, $\alpha_3(M_Z) = 0.11$; (b) $M_{\rm SUSY} = 1$ TeV, $\alpha_3(M_Z) = 0.12$.

TABLE IV. Maximum values of $m_b(m_b)$ in GeV consistent with the 90% confidence levels of $|V_{cb}|$ and $m_c(m_c)$.

$M_{\rm SUSY}$ \ $\alpha_3(M_Z)$	0.11	0.12
m_t	4.56	5.28
1 TeV	4.70	5.33

the GUT scale *Ansatz* for $\alpha_3(M_Z) = 0.11$. The largest consistent values of m_b are given in Table IV.

With $\alpha_3(M_Z) = 0.12$, $|V_{cb}|$ can be much closer to its central value, enhancing the plausibility of the **U** model, with the only caveat being that low m_b ($\lesssim 4.2$ GeV) values produce $\lambda_t(M_G)$ values which are close to being non-perturbative for most values of $\tan\beta$: see Figs. 6(b), 6(d). Notice that the dominant effect of taking the larger value of $\alpha_3(M_Z)$ indicated by two-loop evolution is to increase the QCD-QED scaling factor η_c, thereby allowing $|V_{cb}|$ to be smaller and in better agreement with experiment.

Imposing the constraints on m_b, m_c, and $|V_{cb}|$ also gives the lower limits on the top-quark mass since the $|V_{cb}|$ contours in the smaller $\tan\beta$ region are steeper and eventually cross the m_b/m_τ contours [18]. These lower limits on m_t are summarized in Table V.

The constraints on m_b/m_τ, $|V_{cb}|$ and m_c completely determine the allowed region in the $m_t, \tan\beta$ plane of the **U** model. Other constraints such as the ϵ parameter for CP violation in the neutral kaon system, B mixing or the lighter quark masses affect only the other parameters in the model [18].

If the Yukawa unification is assumed to occur at a scale higher than the gauge couplings, then the predicted value for $|V_{cb}|$ will be lower [4] and easier to reconcile with the experimental data.

B. The D model

Giudice has proposed a different Yukawa mass *Ansatz* [7] of the form

$$\mathbf{U} = \begin{pmatrix} 0 & 0 & b \\ 0 & b & 0 \\ b & 0 & a \end{pmatrix}, \qquad \mathbf{D} = \begin{pmatrix} 0 & fe^{i\phi} & 0 \\ fe^{-i\phi} & d & nd \\ 0 & nd & c \end{pmatrix}, \tag{76}$$

$$\mathbf{E} = \begin{pmatrix} 0 & f & 0 \\ f & -3d & nd \\ 0 & nd & c \end{pmatrix}. \tag{77}$$

TABLE V. Minimum values of $m_t(m_t)$ ($\tan\beta$) in GeV consistent with the 90% confidence levels of $m_b(m_b)$, $|V_{cb}|$ and $m_c(m_c)$.

$M_{\rm SUSY}$ \ $\alpha_3(M_Z)$	0.11	0.12
m_t	155 (1.45)	118 (0.75)
1 TeV	151 (1.16)	116 (0.64)

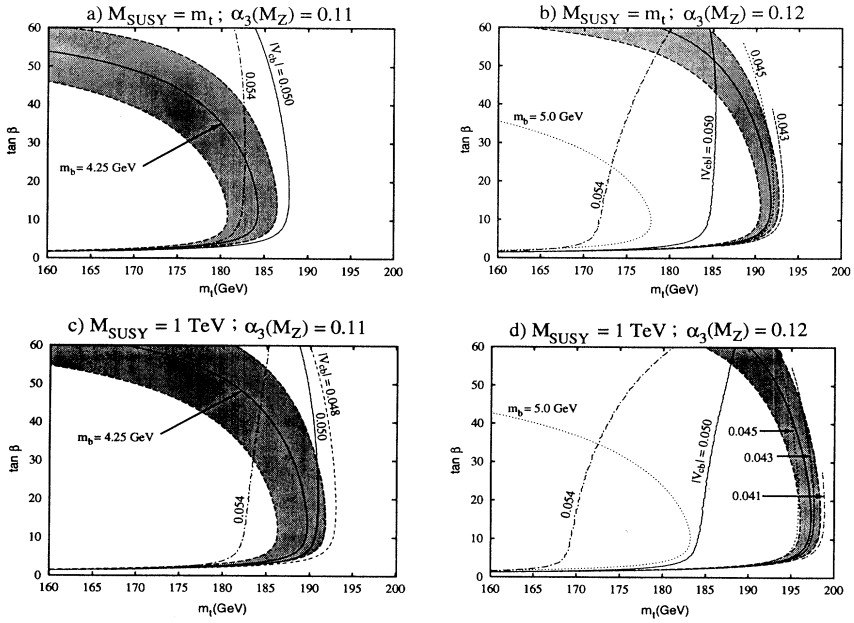

FIG. 10. Comparison of contours for constant $|V_{cb}|$ and constant m_b in the m_t-$\tan\beta$ plane from the RGE's, taking $m_c = 1.27$ GeV, for (a) $M_{\rm SUSY} = m_t$, $\alpha_3(M_Z) = 0.11$; (b) $M_{\rm SUSY} = m_t$, $\alpha_3(M_Z) = 0.12$; (c) $M_{\rm SUSY} = 1$ TeV, $\alpha_3(M_Z) = 0.11$; (d) $M_{\rm SUSY} = 1$ TeV, $\alpha_3(M_Z) = 0.12$. The shaded band indicates the region where the 90% confidence limit is satisfied for m_b. The rightmost contours are discontinued when $\lambda_t(M_G)$ exceeds 6.

This model uses a geometric mean relation $m_c^2 \approx m_u m_t$ at the GUT scale to eliminate one parameter in the up-quark Yukawa matrix. The down-quark Yukawa matrix must then generate the mixing between the second and third generations to get a value for $|V_{cb}|$ that agrees with experiment. Giudice sets the parameter n in the above mass matrices to be 2. We see no *a priori* reason to suppose that this parameter must be an integer and treat it as a free parameter.

We find the generalized one-loop solutions (neglecting λ_b and λ_τ in the RGE's)

$$|V_{us}| = 3\sqrt{\frac{m_e}{m_\mu}}\left(1 - \frac{25}{2}\frac{m_e}{m_\mu} + \frac{4n^2}{9}\frac{m_\mu}{m_\tau}\frac{\eta_\tau}{\eta_\mu}\right), \tag{78}$$

$$|V_{cb}| = \frac{n}{3y}\frac{m_\mu}{m_\tau}\frac{\eta_\tau}{\eta_\mu}\left(1 - \frac{m_e}{m_\mu} + \frac{(n^2-3)}{9}\frac{m_\mu}{m_\tau}\frac{\eta_\tau}{\eta_\mu}\right), \tag{79}$$

$$|V_{ub}| = \frac{y^2}{\eta_c}\frac{m_c}{m_t}, \tag{80}$$

$$m_u = y^3\frac{\eta_u}{\eta_c^2}\frac{m_c^2}{m_t}, \tag{81}$$

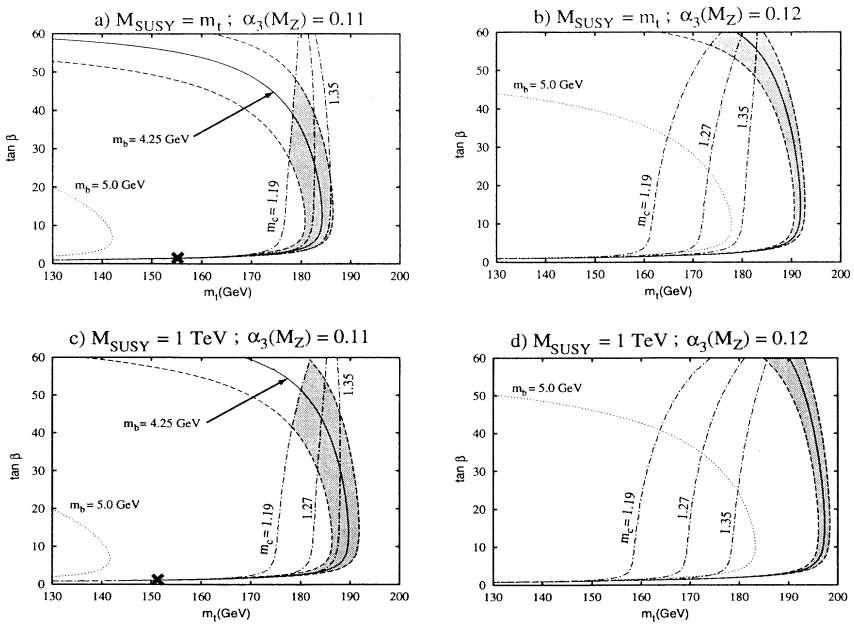

FIG. 11. Comparison of contours for constant m_c and constant m_b in the m_t-$\tan\beta$ plane from the RGE's, taking $|V_{cb}|$ equal to its upper limit 0.54, for (a) $M_{\rm SUSY} = m_t$, $\alpha_3(M_Z) = 0.11$; (b) $M_{\rm SUSY} = m_t$, $\alpha_3(M_Z) = 0.12$; (c) $M_{\rm SUSY} = 1$ TeV, $\alpha_3(M_Z) = 0.11$; (d) $M_{\rm SUSY} = 1$ TeV, $\alpha_3(M_Z) = 0.12$. The shaded band indicates the region where 90% confidence limits are satisfied for all three constraints: m_b, m_c, and $|V_{cb}|$. An **X** marks the lower limit of this shaded band and corresponds to the values in Table V.

$$m_d = \frac{\eta^{1/2}}{x}\frac{\eta_d}{\eta_e}3m_e\left(1 - 8\frac{m_e}{m_\mu} + \frac{4n^2}{9}\frac{m_\mu}{m_\tau}\frac{\eta_\tau}{\eta_\mu}\right), \quad (82)$$

$$m_s = \frac{\eta^{1/2}}{x}\frac{\eta_s}{\eta_\mu}\frac{m_\mu}{3}\left(1 + 8\frac{m_e}{m_\mu} - \frac{4n^2}{9}\frac{m_\mu}{m_\tau}\frac{\eta_\tau}{\eta_\mu}\right), \quad (83)$$

$$m_b = y\frac{\eta^{1/2}}{x}\frac{\eta_b}{\eta_\tau}m_\tau . \quad (84)$$

Notice that at one-loop level to leading order in the mass heirarchy the running $|V_{cb}|$ is related to the strange- and bottom-quark Yukawa couplings by

$$|V_{cb}(\mu)| = nR_{s/b}(\mu) \equiv n\frac{\lambda_s(\mu)}{\lambda_b(\mu)} . \quad (85)$$

Equations (78)–(84) can be compared to Eqs. (58)–(63) for the **U** model, except that we have retained the highest non-leading-order corrections only for the **D** model. When $n = 2$ the predicted value of $|V_{cb}|$ agrees well with the experimental value. On the other hand $|V_{us}|$ is just at the lower limit of its 90% confidence level. The overall situation can be improved somewhat by allowing n to be slightly larger than 2.

The leading term in Eq. (78) can be recognized as the relation [19] between the Cabibbo angle and the quark masses, $\tan\theta_C \approx \sqrt{m_d/m_s}$, supplemented by the Yukawa unification relation $m_d/m_s = 9m_e/m_\mu$. Notice that this relation involving the first and second generations does not run, so the prediction of the Cabibbo angle is insensitive to the size of the gauge and Yukawa couplings. The two-loop effects for the most part increase α_3 and hence the QCD scaling factors η_q. The influence of two-loop contributions in the running of the Yukawa couplings is small.

For $\tan\beta \lesssim 10$, λ_b and λ_τ can be neglected in the RGE's; then the relation for m_u in Eq. (81) implies an upper limit on m_t [7]. However, further solutions for m_b/m_τ are possible with large $\tan\beta$, as can be seen in Fig. 5. In the allowed m_b/m_τ band at large $\tan\beta$ the predicted value for m_u from Eq. (81) is still satisfactory, since m_t is in the same range as found for the small $\tan\beta$ solutions.

The CP-violating phase is not very well constrained in the **D** model since the phase does not enter in the well-measured CKM elements; in fact the phase can assume almost any nonzero value within its zero to 2π range. Correspondingly CP asymmetries to be measured in B decays are not very constrained in the model [48]. In contrast, the CP-violating phase in the **U** model is almost uniquely determined by $|V_{us}|$ and the CP-violating asymmetries are predicted precisely. This remains the case at the two-loop level. In the **U** model scheme the dependence on $\alpha_3(M_Z)$ cancels out in quark mass ratios, and since the constraint on the phase arises from the first- and second-generation mixing angles, there is no dependence of the phase on λ_t.

V. CONCLUSION

We have investigated unification scenarios in supersymmetric grand unified theories using the two-loop renormalization-group equations. Our primary conclusions are the following:

(1) Given the experimentally determined values for α_1 and α_2 at M_Z, the RGE's predict $\alpha_3 \simeq 0.111(0.122)$ at one-loop (two-loop) for $M_{\rm SUSY} = m_t$ and $\alpha_3 \simeq 0.106(0.116)$ for $M_{\rm SUSY} = 1$ TeV. Including the Yukawa couplings in the two-loop evolution of the gauge couplings decreases $\alpha_3(M_Z)$ by only a few percent. Thus the values of $\alpha_3(M_Z) \simeq 0.12$ obtained experimentally at LEP II are also theoretically preferred if GUT-scale thresholds effects or intermediate scales are not important.

(2) For any fixed value of $\alpha_3(M_Z)$ and m_b there are just two allowed solutions for $\tan\beta$ for a given top-quark mass if $m_t \lesssim 180$ GeV; the larger solution has $\tan\beta > m_t/m_b$ and the smaller solution is $\sin\beta \simeq 0.78(m_t/150\ \text{GeV})$. Allowing for some uncertainty in $\alpha_3(M_Z)$, m_b, and $M_{\rm SUSY}$, these unique solutions for $\tan\beta$ at given m_t become a narrow range of values. For $m_t \approx 180 - 200$ GeV the value of $\tan\beta$ changes rapidly with m_t.

(3) With λ_b, λ_τ unification we find an upper limit $m_t \lesssim 200$ GeV on the top-quark mass by requiring the successful prediction of the m_b/m_τ ratio; we also obtain lower limits $m_t \gtrsim 150$ GeV (115 GeV) for $\alpha_3(M_Z) = 0.11(0.12)$ from evolution constraints on m_b, m_c and $|V_{cb}|$. These lower limits are only mildly sensitive to $M_{\rm SUSY}$.

(4) The effects of raising $M_{\rm SUSY}$ is to decrease both α_G and M_G and to decrease the values of $\alpha_3(M_Z)$ that yield successful unification. Also, the allowed band for the m_b/m_τ ratio in the m_t-$\tan\beta$ plane is shifted towards slightly higher top-quark masses. This in turn slightly reduces the prediction for $|V_{cb}|$ in models that utilize the relation $\sqrt{\lambda_c(M_G)/\lambda_t(M_G)} = |V_{cb}(M_G)|$.

(5) In the **U** model we find an upper limit on the supersymmetry parameter $\tan\beta \lesssim 50(60)$ for $M_{\rm SUSY} = m_t(1\ \text{TeV})$ if $\alpha_3(M_Z) \simeq 0.11$; for $\alpha_3(M_Z) = 0.12$ the solutions at large $\tan\beta$ extend into the region for which $\lambda_b(M_G)$ is nonperturbative.

(6) For the value $\alpha_3(M_Z) \simeq 0.12$ indicated by the two-loop RGE's, the agreement of the $|V_{cb}|$ prediction of the **U** *Ansatz* with experiment is improved. In fact for $\alpha_3(M_Z) = 0.12$ and $M_{\rm SUSY} = 1$ TeV the central values for $|V_{cb}|$ and the mass ratio m_b/m_τ almost coincide in the m_t-$\tan\beta$ plane; see Fig. 10(d). This result is more general than the **U** *Ansatz*, and occurs for any model with the GUT-scale relation $|V_{cb}| = \sqrt{\lambda_c/\lambda_t}$.

(7) With $\alpha_3(M_Z) \simeq 0.12$ a large top-quark Yukawa coupling is needed to achieve the correct m_b/m_τ ratio, and the theory is in some jeopardy of having a nonperturbative $\lambda_t(M_G)$ if m_b is smaller than about 4.2 GeV.

(8) GUT unification of λ_τ, λ_b, and λ_t can be realized for $\tan\beta \gtrsim 50$.

(9) The predictions for the CP asymmetries in the **U** model are largely unaffected by our two-loop analysis.

(10) We have found new solutions to the **D** model for large $\tan\beta$. These results require the inclusion of λ_b and λ_τ in the RGE's, and therefore could not be obtained in Giudice's analytic treatment at one loop.

ACKNOWLEDGMENTS

One of us (V.B.) thanks Pierre Ramond for a discussion. One of us (M.B.) thanks Greg Anderson for a discussion. We thank Tao Han for his participation in the initial stages of this project. This research was supported in part by the University of Wisconsin Research Committee with funds granted by the Wisconsin Alumni Research Foundation, in part by the U.S. Department of Energy under Contract No. DE-AC02-76ER00881, and in part by the Texas National Laboratory Research Commission under Grant No. RGFY9273. Further support was also provided by the U.S. Department of Education under Grant No. P200A80214. P.O. was supported in part by the NSF Graduate Program.

APPENDIX

To consider a specific *Ansatz* for Yukawa matrices at the GUT scale at the two-loop level requires knowledge of the RGE's. These can be derived from formal expressions that exist in the literature [27]. For the supersymmetric model with two Higgs doublets, the one- [26] and two-loop RGE's can be written for general Yukawa matrices as

$$\frac{dg_i}{dt} = \frac{g_i}{16\pi^2}\left[b_i g_i^2 + \frac{1}{16\pi^2}\left(\sum_{j=1}^{3} b_{ij} g_i^2 g_j^2 - \sum_{j=U,D,E} a_{ij} g_i^2 \mathrm{Tr}[\mathbf{Y_j Y_j^\dagger}]\right)\right], \tag{A1}$$

with $\mathbf{Y_U} \equiv \mathbf{U}$, etc.,

$$\begin{aligned}\frac{d\mathbf{U}}{dt} = \frac{1}{16\pi^2}\Bigg[&\Big[-\sum c_i g_i^2 + 3\mathbf{U}\mathbf{U}^\dagger + \mathbf{D}\mathbf{D}^\dagger + \mathrm{Tr}[3\mathbf{U}\mathbf{U}^\dagger]\Big] \\ &+\frac{1}{16\pi^2}\Bigg(\sum\left(c_i b_i + c_i^2/2\right) g_i^4 + g_1^2 g_2^2 + \frac{136}{45} g_1^2 g_3^2 + 8 g_2^2 g_3^2 \\ &\quad + \left(\frac{2}{5}g_1^2 + 6g_2^2\right)\mathbf{U}\mathbf{U}^\dagger + \frac{2}{5}g_1^2 \mathbf{D}\mathbf{D}^\dagger + \left(\frac{4}{5}g_1^2 + 16 g_3^2\right)\mathrm{Tr}[\mathbf{U}\mathbf{U}^\dagger] \\ &\quad -9\mathrm{Tr}[\mathbf{U}\mathbf{U}^\dagger\mathbf{U}\mathbf{U}^\dagger] - 3\mathrm{Tr}[\mathbf{U}\mathbf{U}^\dagger\mathbf{D}\mathbf{D}^\dagger] - 9\mathbf{U}\mathbf{U}^\dagger\mathrm{Tr}[\mathbf{U}\mathbf{U}^\dagger] \\ &\quad -\mathbf{D}\mathbf{D}^\dagger\mathrm{Tr}[3\mathbf{D}\mathbf{D}^\dagger + \mathbf{E}\mathbf{E}^\dagger] - 4(\mathbf{U}\mathbf{U}^\dagger)^2 - 2(\mathbf{D}\mathbf{D}^\dagger)^2 - 2\mathbf{U}\mathbf{U}^\dagger\mathbf{D}\mathbf{D}^\dagger\Bigg)\Bigg]\mathbf{U}\,,\end{aligned} \tag{A2}$$

$$\begin{aligned}\frac{d\mathbf{D}}{dt} = \frac{1}{16\pi^2}\Bigg[&\Big[-\sum c_i' g_i^2 + 3\mathbf{D}\mathbf{D}^\dagger + \mathbf{U}\mathbf{U}^\dagger + \mathrm{Tr}[3\mathbf{D}\mathbf{D}^\dagger + \mathbf{E}\mathbf{E}^\dagger]\Big] \\ &+\frac{1}{16\pi^2}\Bigg(\sum\left(c_i' b_i + c_i'^2/2\right) g_i^4 + g_1^2 g_2^2 + \frac{8}{9} g_1^2 g_3^2 + 8 g_2^2 g_3^2 \\ &\quad + \left(\frac{4}{5}g_1^2 + 6g_2^2\right)\mathbf{D}\mathbf{D}^\dagger + \frac{4}{5}g_1^2 \mathbf{U}\mathbf{U}^\dagger + \left(-\frac{2}{5}g_1^2 + 16 g_3^2\right)\mathrm{Tr}[\mathbf{D}\mathbf{D}^\dagger] + \frac{6}{5}g_1^2\mathrm{Tr}[\mathbf{E}\mathbf{E}^\dagger] \\ &\quad -9\mathrm{Tr}[\mathbf{D}\mathbf{D}^\dagger\mathbf{D}\mathbf{D}^\dagger] - 3\mathrm{Tr}[\mathbf{D}\mathbf{D}^\dagger\mathbf{U}\mathbf{U}^\dagger] - 3\mathrm{Tr}[\mathbf{E}\mathbf{E}^\dagger\mathbf{E}\mathbf{E}^\dagger] - 3\mathbf{U}\mathbf{U}^\dagger\mathrm{Tr}[\mathbf{U}\mathbf{U}^\dagger] \\ &\quad -3\mathbf{D}\mathbf{D}^\dagger\mathrm{Tr}[3\mathbf{D}\mathbf{D}^\dagger + \mathbf{E}\mathbf{E}^\dagger] - 4(\mathbf{D}\mathbf{D}^\dagger)^2 - 2(\mathbf{U}\mathbf{U}^\dagger)^2 - 2\mathbf{D}\mathbf{D}^\dagger\mathbf{U}\mathbf{U}^\dagger\Bigg)\Bigg]\mathbf{D}\,,\end{aligned} \tag{A3}$$

$$\begin{aligned}\frac{d\mathbf{E}}{dt} = \frac{1}{16\pi^2}\Bigg[&\Big[-\sum c_i'' g_i^2 + 3\mathbf{E}\mathbf{E}^\dagger + \mathrm{Tr}[3\mathbf{D}\mathbf{D}^\dagger + \mathbf{E}\mathbf{E}^\dagger]\Big] \\ &+\frac{1}{16\pi^2}\Bigg(\sum\left(c_i'' b_i + c_i''^2/2\right) g_i^4 + \frac{9}{5} g_1^2 g_2^2 + 6 g_2^2 \mathbf{E}\mathbf{E}^\dagger + \left(-\frac{2}{5}g_1^2 + 16 g_3^2\right)\mathrm{Tr}[\mathbf{D}\mathbf{D}^\dagger] + \frac{6}{5}g_1^2\mathrm{Tr}[\mathbf{E}\mathbf{E}^\dagger] \\ &\quad -9\mathrm{Tr}[\mathbf{D}\mathbf{D}^\dagger\mathbf{D}\mathbf{D}^\dagger] - 3\mathrm{Tr}[\mathbf{D}\mathbf{D}^\dagger\mathbf{U}\mathbf{U}^\dagger] - 3\mathrm{Tr}[\mathbf{E}\mathbf{E}^\dagger\mathbf{E}\mathbf{E}^\dagger] \\ &\quad -3\mathbf{E}\mathbf{E}^\dagger\mathrm{Tr}[3\mathbf{D}\mathbf{D}^\dagger + \mathbf{E}\mathbf{E}^\dagger] - 4(\mathbf{E}\mathbf{E}^\dagger)^2\Bigg)\Bigg]\mathbf{E}\,,\end{aligned} \tag{A4}$$

where

$$b_i = \left(\frac{33}{5}, 1, -3\right) , \tag{A5}$$

$$c_i = \left(\frac{13}{15}, 3, \frac{16}{3}\right) , \tag{A6}$$

$$c_i' = \left(\frac{7}{15}, 3, \frac{16}{3}\right) , \tag{A7}$$

$$c_i'' = \left(\frac{9}{5}, 3, 0\right) , \tag{A8}$$

$$d_i = c_i' - c_i'' , \tag{A9}$$

$$b_{ij} = \begin{pmatrix} \frac{199}{25} & \frac{27}{5} & \frac{88}{5} \\ \frac{9}{5} & 25 & 24 \\ \frac{11}{5} & 9 & 14 \end{pmatrix} , \tag{A10}$$

and

$$a_{ij} = \begin{pmatrix} \frac{26}{5} & \frac{14}{5} & \frac{18}{5} \\ 6 & 6 & 2 \\ 4 & 4 & 0 \end{pmatrix} . \tag{A11}$$

These equations agree with those in the last paper in Ref. [27] for the case where the Yukawa matrices are diagonal, if the following minor corrections are made: (1) b_{31} should be decreased by a factor 3; (2) the closing parenthesis in the second term of $\gamma_{H_2}^{(2)}$ should come before the α_2^2; (3) the first term of $\gamma_{\bar{\tau}}^{(2)}$ should have a factor α_1^2 instead of α_2^2.

The two-loop RGE's for the standard model are [28]

$$\frac{dg_i}{dt} = \frac{g_i}{16\pi^2}\left[b_i^{\rm SM} g_i^2 + \frac{1}{16\pi^2}\left(\sum_{j=1}^{3} b_{ij}^{\rm SM} g_i^2 g_j^2 - \sum_{j=U,D,E} a_{ij}^{\rm SM} g_i^2 {\rm Tr}[\mathbf{Y_j Y_j^\dagger}]\right)\right] , \tag{A12}$$

$$\begin{aligned} \frac{d\mathbf{U}}{dt} = \frac{1}{16\pi^2}\Bigg[& \Big[-\sum c_i^{\rm SM} g_i^2 + \frac{3}{2}\mathbf{U}\mathbf{U}^\dagger - \frac{3}{2}\mathbf{D}\mathbf{D}^\dagger + Y_2(S)\Big] \\ & + \frac{1}{16\pi^2}\Bigg(\frac{1187}{600} g_1^4 - \frac{23}{4} g_2^4 - 108 g_3^4 - \frac{9}{20} g_1^2 g_2^2 + \frac{19}{15} g_1^2 g_3^2 + 9 g_2^2 g_3^2 \\ & + \left(\frac{223}{80} g_1^2 + \frac{135}{16} g_2^2 + 16 g_3^2\right)\mathbf{U}\mathbf{U}^\dagger - \left(\frac{43}{80} g_1^2 - \frac{9}{16} g_2^2 + 16 g_3^2\right)\mathbf{D}\mathbf{D}^\dagger \\ & + \frac{5}{2} Y_4(S) - 2\lambda\left(3\mathbf{U}\mathbf{U}^\dagger + \mathbf{D}\mathbf{D}^\dagger\right) + \frac{3}{2}(\mathbf{U}\mathbf{U}^\dagger)^2 - \mathbf{D}\mathbf{D}^\dagger\mathbf{U}\mathbf{U}^\dagger - \frac{1}{4}\mathbf{U}\mathbf{U}^\dagger\mathbf{D}\mathbf{D}^\dagger + \frac{11}{4}(\mathbf{D}\mathbf{D}^\dagger)^2 \\ & + Y_2(S)\left(\frac{5}{4}\mathbf{D}\mathbf{D}^\dagger - \frac{9}{4}\mathbf{U}\mathbf{U}^\dagger\right) - \chi_4(S) + \frac{3}{2}\lambda^2\Bigg)\Bigg]\mathbf{U} , \end{aligned} \tag{A13}$$

$$\begin{aligned} \frac{d\mathbf{D}}{dt} = \frac{1}{16\pi^2}\Bigg[& \Big[-\sum c_i'^{\rm SM} g_i^2 + \frac{3}{2}\mathbf{D}\mathbf{D}^\dagger - \frac{3}{2}\mathbf{U}\mathbf{U}^\dagger + Y_2(S)\Big] \\ & + \frac{1}{16\pi^2}\Bigg(-\frac{127}{600} g_1^4 - \frac{23}{4} g_2^4 - 108 g_3^4 - \frac{27}{20} g_1^2 g_2^2 + \frac{31}{15} g_1^2 g_3^2 + 9 g_2^2 g_3^2 \\ & - \left(\frac{79}{80} g_1^2 - \frac{9}{16} g_2^2 + 16 g_3^2\right)\mathbf{U}\mathbf{U}^\dagger + \left(\frac{187}{80} g_1^2 + \frac{135}{16} g_2^2 + 16 g_3^2\right)\mathbf{D}\mathbf{D}^\dagger \\ & + \frac{5}{2} Y_4(S) - 2\lambda\left(\mathbf{U}\mathbf{U}^\dagger + 3\mathbf{D}\mathbf{D}^\dagger\right) + \frac{3}{2}(\mathbf{D}\mathbf{D}^\dagger)^2 - \mathbf{U}\mathbf{U}^\dagger\mathbf{D}\mathbf{D}^\dagger - \frac{1}{4}\mathbf{D}\mathbf{D}^\dagger\mathbf{U}\mathbf{U}^\dagger + \frac{11}{4}(\mathbf{U}\mathbf{U}^\dagger)^2 \\ & + Y_2(S)\left(\frac{5}{4}\mathbf{U}\mathbf{U}^\dagger - \frac{9}{4}\mathbf{D}\mathbf{D}^\dagger\right) - \chi_4(S) + \frac{3}{2}\lambda^2\Bigg)\Bigg]\mathbf{D} , \end{aligned} \tag{A14}$$

$$\frac{d\mathbf{E}}{dt}=\frac{1}{16\pi^2}\Bigg[\Big[-\sum c_i''^{\mathrm{SM}}g_i^2+\frac{3}{2}\mathbf{E}\mathbf{E}^\dagger+Y_2(S)\Big]$$
$$+\frac{1}{16\pi^2}\left(\frac{1371}{200}g_1^4-\frac{23}{4}g_2^4+\frac{27}{20}g_1^2g_2^2+\left(\frac{387}{80}g_1^2+\frac{135}{16}g_2^2\right)\mathbf{E}\mathbf{E}^\dagger+\frac{5}{2}Y_4(S)-6\lambda\mathbf{E}\mathbf{E}^\dagger\right.$$
$$\left.+\frac{3}{2}(\mathbf{E}\mathbf{E}^\dagger)^2-\frac{9}{4}Y_2(S)\mathbf{E}\mathbf{E}^\dagger-\chi_4(S)+\frac{3}{2}\lambda^2\right)\Bigg]\mathbf{E}\,, \tag{A15}$$

$$\frac{d\lambda}{dt}=\frac{1}{16\pi^2}\Bigg[\left\{\frac{9}{4}\left(\frac{3}{25}g_1^4+\frac{2}{5}g_1^2g_2^2+g_2^4\right)-\left(\frac{9}{5}g_1^2+9g_2^2\right)\lambda+4Y_2(S)\lambda-4H(S)+12\lambda^2\right\}$$
$$+\frac{1}{16\pi^2}\left(-78\lambda^3+18\left(\frac{3}{5}g_1^2+3g_2^2\right)\lambda^2+\left(-\frac{73}{8}g_2^4+\frac{117}{20}g_1^2g_2^2+\frac{1887}{200}g_1^4\right)\lambda\right.$$
$$+\frac{305}{8}g_2^6-\frac{867}{120}g_1^2g_2^4-\frac{1677}{200}g_1^4g_2^2-\frac{3411}{1000}g_1^6-64g_3^2\mathrm{Tr}[(\mathbf{U}\mathbf{U}^\dagger)^2+(\mathbf{D}\mathbf{D}^\dagger)^2]$$
$$-\frac{8}{5}g_1^2\mathrm{Tr}[2(\mathbf{U}\mathbf{U}^\dagger)^2-(\mathbf{D}\mathbf{D}^\dagger)^2+3(\mathbf{E}\mathbf{E}^\dagger)^2]-\frac{3}{2}g_2^4Y_2(S)+10\lambda Y_4(S)$$
$$+\frac{3}{5}g_1^2\left[\left(-\frac{57}{10}g_1^2+21g_2^2\right)\mathrm{Tr}[\mathbf{U}\mathbf{U}^\dagger]+\left(\frac{3}{2}g_1^2+9g_2^2\right)\mathrm{Tr}[\mathbf{D}\mathbf{D}^\dagger]\right.$$
$$\left.+\left(-\frac{15}{2}g_1^2+11g_2^2\right)\mathrm{Tr}[\mathbf{E}\mathbf{E}^\dagger]\right]-24\lambda^2Y_2(S)-\lambda H(S)+6\lambda\mathrm{Tr}[\mathbf{U}\mathbf{U}^\dagger\mathbf{D}\mathbf{D}^\dagger]$$
$$\left.+20\mathrm{Tr}\left[3(\mathbf{U}\mathbf{U}^\dagger)^3+3(\mathbf{D}\mathbf{D}^\dagger)^3+(\mathbf{E}\mathbf{E}^\dagger)^3\right]-12\mathrm{Tr}\left[\mathbf{U}\mathbf{U}^\dagger(\mathbf{U}\mathbf{U}^\dagger+\mathbf{D}\mathbf{D}^\dagger)\mathbf{D}\mathbf{D}^\dagger\right]\right)\Bigg]\,, \tag{A16}$$

where

$$b_i^{\mathrm{SM}}=\left(\frac{41}{10},-\frac{19}{6},-7\right)\,, \tag{A17}$$
$$c_i^{\mathrm{SM}}=\left(\frac{17}{20},\frac{9}{4},8\right)\,, \tag{A18}$$
$$c_i'^{\mathrm{SM}}=\left(\frac{1}{4},\frac{9}{4},8\right)\,, \tag{A19}$$
$$c_i''^{\mathrm{SM}}=\left(\frac{9}{4},\frac{9}{4},0\right)\,, \tag{A20}$$
$$Y_2(S)=\mathrm{Tr}[3\mathbf{U}\mathbf{U}^\dagger+3\mathbf{D}\mathbf{D}^\dagger+\mathbf{E}\mathbf{E}^\dagger]\,, \tag{A21}$$
$$Y_4(S)=\frac{1}{3}\left[3\sum c_i^{\mathrm{SM}}g_i^2\mathrm{Tr}[\mathbf{U}\mathbf{U}^\dagger]+3\sum c_i'^{\mathrm{SM}}g_i^2\mathrm{Tr}[\mathbf{D}\mathbf{D}^\dagger]+\sum c_i''^{\mathrm{SM}}g_i^2\mathrm{Tr}[\mathbf{E}\mathbf{E}^\dagger]\right]\,, \tag{A22}$$
$$\chi_4(S)=\frac{9}{4}\mathrm{Tr}\left[3(\mathbf{U}\mathbf{U}^\dagger)^2+3(\mathbf{D}\mathbf{D}^\dagger)^2+(\mathbf{E}\mathbf{E}^\dagger)^2-\frac{2}{3}\mathbf{U}\mathbf{U}^\dagger\mathbf{D}\mathbf{D}^\dagger\right]\,, \tag{A23}$$
$$H(S)=\mathrm{Tr}[3(\mathbf{U}\mathbf{U}^\dagger)^2+3(\mathbf{D}\mathbf{D}^\dagger)^2+(\mathbf{E}\mathbf{E}^\dagger)^2]\,, \tag{A24}$$
$$b_{ij}^{\mathrm{SM}}=\begin{pmatrix}\frac{199}{50}&\frac{27}{10}&\frac{44}{5}\\ \frac{9}{10}&\frac{35}{6}&12\\ \frac{11}{10}&\frac{9}{2}&-26\end{pmatrix}\,, \tag{A25}$$

and

$$a_{ij}^{\mathrm{SM}}=\begin{pmatrix}\frac{17}{10}&\frac{1}{2}&\frac{3}{2}\\ \frac{3}{2}&\frac{3}{2}&\frac{1}{2}\\ 2&2&0\end{pmatrix}\,. \tag{A26}$$

These renormalization-group equations are those given in the classic papers of Machacek and Vaughn after replacing $\mathbf{H} \to \mathbf{U}^\dagger$, $\mathbf{F}_D \to \mathbf{D}^\dagger$, $\mathbf{F}_L \to \mathbf{E}^\dagger$, and making the following corrections to Eq. (A16) mentioned in the paper of Ford, Jack, and Jones [28]: (1) The λg_2^2 term in the one-loop β function has a coefficient 9 instead of 1. (2) The $\lambda g_1^2 g_2^2$ term in the two-loop β function has a coefficient $+117/20$ instead of $-117/20$. (3) The λg_1^4 in the two-loop β function has a coefficient $+1887/200$ instead of $-1119/200$.

[1] For review and references see, e.g., R. Mohapatra, *Unification and Supersymmetry*, 2nd ed. (Springer-Verlag, Berlin, 1992); G. G. Ross, *Grand Unified Theories* (Addison-Wesley, Reading, MA, 1984).

[2] U. Amaldi, Wim de Boer, and H. Furstenau, Phys. Lett. B **260**, 447 (1991); J. Ellis, S. Kelley, and D. V. Nanopoulos, *ibid.* **260**, 131 (1991); P. Langacker and M. Luo, Phys. Rev. D **44**, 817 (1991).

[3] U. Amaldi *et al.*, Phys. Rev. D **36**, 1385 (1987); G. Costa, J. Ellis, G. L. Fogli, D. V. Nanopoulos, and F. Zwirner, Nucl. Phys. **B297**, 244 (1988); J. Ellis, S. Kelley, and D. V. Nanopoulos, Phys. Lett. B **249**, 442 (1990); S. Kelley, J. L. Lopez, D. V. Nanopoulos, H. Pois, and K. Yuan, *ibid.* **249**, 423 (1991); F. Anselmo, L. Cifarelli, A. Petermann, and A. Zichichi, Nuovo Cimento **104A**, 1817 (1991); J. Ellis, S. Kelley, and D. V. Nanopoulos, Phys. Lett. B **287**, 95 (1992).

[4] H. Arason, D. J. Castaño, B. Keszthelyi, S. Mikaelian, E. J. Piard, P. Ramond, and B. D. Wright, Phys. Rev. Lett. **67**, 2933 (1991); P. Ramond, University of Florida Report No. UFIFT-92-4 (unpublished); H. Arason, D. J. Castaño, E. J. Piard, and P. Ramond, Phys. Rev. D **47**, 232 (1993).

[5] H. Arason, D. J. Castaño, B. Keszthelyi, S. Mikaelian, E. J. Piard, P. Ramond, and B. D. Wright, Phys. Rev. D **46**, 3945 (1992).

[6] S. Dimopoulos, L. J. Hall, and S. Raby, Phys. Rev. Lett. **68**, 1984 (1992); Phys. Rev. D **45**, 4192 (1992).

[7] G. F. Giudice, Mod. Phys. Lett. A **7**, 2429 (1992).

[8] B. R. Greene, K. H. Kirklin, P. J. Miron, and G. G. Ross, Nucl. Phys. **B292**, 606 (1987); J. L. Lopez and D. V. Nanopoulos, Phys. Lett. B **251**, 73 (1990); J. A. Casas and C. Muñoz, Nucl. Phys. **B322**, 189 (1990); F. del Aguila, M. Masip, and L. A. C. P. da Mota, Phys. Lett. B **287**, 335 (1992); K. S. Babu and Q. Shafi, Bartol Research Institute Report No. BA-92-27, 1992 (unpublished).

[9] G. G. Ross and R. G. Roberts, Nucl. Phys. **B377**, 571 (1992); R. Arnowitt and P. Nath, Phys. Rev. Lett. **69**, 725 (1992); S. Kelley, J. L. Lopez, D. V. Nanopoulos, H. Pois, and K. Yuan, CERN Report No. CERN-TH.6498/92, 1992 (unpublished).

[10] See, e.g., S. Bethke and S. Catani, Report No. CERN-TH.6484/92, 1992 (unpublished); S. Bethke, presented at the Proceedings of the XXVI International Conference on High Energy Physics, Dallas, Texas 1992 (unpublished).

[11] Particle Data Group, K. Hikasa *et al.*, Phys. Rev. D **45**, S1 (1992).

[12] J. Ellis, D. V. Nanopoulos, and S. Rudaz, Nucl. Phys. **B202**, 43 (1982); R. Arnowitt and P. Nath, Northeastern University Report No. NUB-TH-3051-92, 1992 (unpublished); J. L. Lopez, D. V. Nanopoulos, and A. Zichichi, CERN Report No. CERN-TH.6554/92, 1992 (unpublished); J. Hisano, H. Murayama, and T. Yanagida, Phys. Rev. Lett. **69**, 1014 (1992); Tohoku University Report No. TU-400, 1992 (unpublished).

[13] H. Georgi and S. Glashow, Phys. Rev. Lett. **32**, 438 (1974); H. Georgi, H. Quinn, and S. Weinberg, *ibid.* **33**, 451 (1974); S. Dimopoulos, S. Raby, and F. Wilczek, Phys. Rev. D **24**, 1681 (1981); S. Dimopoulos and H. Georgi, Nucl. Phys. **B293**, 150 (1981); N. Sakai, Z. Phys. C **11**, 153 (1981).

[14] M. Chanowitz, J. Ellis, and M. Gaillard, Nucl. Phys. **B128**, 506 (1977); A. Buras, J. Ellis, M. Gaillard, and D. Nanopoulos, *ibid.* **B135**, 66 (1978).

[15] M. B. Einhorn and D. R. T. Jones, Nucl. Phys. **B196**, 475 (1982); J. Ellis, D. V. Nanopoulos, and S. Rudaz, *ibid.* **B202**, 43 (1982).

[16] J. Harvey, P. Ramond, and D. B. Reiss, Phys. Lett. **92B**, 309 (1980); Nucl. Phys. **B199**, 223 (1982).

[17] S. Kelley, J. L. Lopez, and D. V. Nanopoulos, Phys. Lett. B **274**, 387 (1992); J. Ellis, S. Kelley, and D. V. Nanopoulos, Nucl. Phys. **B373**, 55 (1992).

[18] V. Barger, M. S. Berger, T. Han, and M. Zralek, Phys. Rev. Lett. **68**, 3394 (1992).

[19] R. Gatto, G. Sartori, and M. Tonin, Phys. Lett. **28B**, 128 (1968); N. Cabibbo and L. Maiani, *ibid.* **28B**, 131 (1968); R. J. Oakes, *ibid.* **29B**, 683 (1969).

[20] S. Weinberg, *A Festschrift for I. I. Rabi* (New York Academy of Sciences, New York, 1977); F. Wilczek and A. Zee, Phys. Lett. **70B**, 418 (1977).

[21] H. Fritzsch, Phys. Lett. **70B**, 436 (1977); **73B**, 317 (1978); Nucl. Phys. **B155**, 189 (1979).

[22] H. Georgi and C. Jarlskog, Phys. Lett. **86B**, 297 (1979).

[23] H. Georgi and D. Nanopoulos, Nucl. Phys. **B159**, 16 (1979).

[24] A. C. Rothman and K. Kang, Phys. Rev. Lett. **43**, 1548 (1979); B. Stech, Phys. Lett. **130B**, 189 (1983); M. Shin, *ibid.* **145B**, 285 (1984); M. Gronau, R. Johnson, and J. Schechter, Phys. Rev. Lett. **54**, 2176 (1985); H. Fritzsch, Phys. Lett. **166B**, 423 (1986); M. Soldate, M. H. Reno, and C. T. Hill, Phys. Lett. B **179**, 95 (1986); R. Johnson, J. Schechter, and M. Gronau, Phys. Rev. D **33**, 2641 (1987); M. Tanimoto and A. Takatsu, *ibid.* **34**, 1474 (1986); F. del Aguila, G. L. Kane, and M. Quiros, Phys. Lett. B **196**, 531 (1987); C. H. Albright, C. Jarlskog, and B. Lindholm, *ibid.* **199**, 553 (1987); Phys. Rev. D **38**, 872 (1988); K. Kang and S. Hadjitheodoridis, Phys. Lett. B **193**, 504 (1987); M. Gronau, R. Johnson, and J. Schechter, *ibid.* **201**, 151 (1988); C. H. Albright, *ibid.* **224**, 213 (1989); H. P. Nilles, M. Olechowski, and S. Pokorski, *ibid.* **228**, 406 (1989); X. G. He and W. S. Hou, Phys. Rev. D **41**, 1517 (1990); P. Kaus and S. Meshkov, *ibid.* **42**, 1863 (1990); C. H. Albright, Phys. Lett. B **246**, 451 (1990); D. Ng and Y. J. Ng, Mod. Phys. Lett. A **6**, 2243 (1991); K. Kang, J. Flanz, and E. Paschos, Z. Phys. C **55**, 75 (1992); J. L. Rosner and M. Worah, Phys. Rev. D **46**, 1131 (1992).

[25] B. Pendleton and G. G. Ross, Phys. Lett. **98B**, 291 (1981); N. Cabibbo, L. Maiani, G. Parisi, and

R. Petronzio, Nucl. Phys. **B158**, 295 (1979); C. T. Hill, Phys. Rev. D **24**, 691 (1981); E. A. Paschos, Z. Phys. C **26**, 235 (1984); J. W. Halley, E. A. Paschos, and H. Usler, Phys. Lett. **155B**, 107 (1985); J. Bagger, S. Dimopoulos, and E. Masso, Nucl. Phys. **B253**, 397 (1985); M. Tanimoto, T. Hayashi, R. Najima, and S. Wakaizumi, Prog. Theor. Phys. **76**, 1098 (1986); K. S. Babu and E. Ma, Europhys. Lett. **3**, 437 (1987); M. Tanimoto, Y. Suetake, and K. Seuba, Phys. Rev. D **36**, 2119 (1987); C. H. Albright and M. Lindner, Phys. Lett. B **213**, 347 (1988); Z. Phys. C **44**, 673 (1989); E. M. Freire, G. Lazarides, and Q. Shafi, Mod. Phys. Lett. A **5**, 2453 (1990); G. Cvetic and C. S. Kim, Dortmund University Report No. DO-TH-92-08, 1992 (unpublished).

[26] K. Inoue, A. Kakuto, H. Komatsu, and S. Takeshita, Prog. Theor. Phys. **67**, 1889 (1982).

[27] D. R. T. Jones and L. Mezincescu, Phys. Lett. **136B**, 242 (1984); P. West, *ibid.* **137B**, 371 (1984); A. Parkes and P. West, *ibid.* **138B**, 99 (1984); D. R. T. Jones and L. Mezincescu, *ibid.* **138B**, 293 (1984); J. E. Björkman and D. R. T. Jones, Nucl. Phys. **B259**, 533 (1985).

[28] M. E. Machacek and M. T. Vaughn, Nucl. Phys. **B222**, 83 (1983); **B236**, 221 (1984); **B249**, 70 (1985); M. Fischler and J. Oliensis, Phys. Lett. **119B**, 385 (1982); Phys. Rev D **28**, 2027 (1983); I. Jack, J. Phys. A **16**, 1083 (1983); I. Jack and H. Osborn, *ibid.* **16**, 1101 (1983); I. Jack, Phys. Lett. **147B**, 405 (1984); I. Jack and H. Osborn, Nucl. Phys. **B249**, 472 (1985); C. Ford, I. Jack, and D. R. T. Jones, Report No. NSF-ITP-92-21, 1992 (unpublished).

[29] P. Langacker, University of Pennsylvania Report No. UPR-0492T, 1992 (unpublished).

[30] A. Sirlin, Nucl. Phys. **B332**, 20 (1990); P. Langacker, Phys. Rep. **72**, 185 (1981); A. Buras, Rev. Mod. Phys. **52**, 199 (1980); G. 't Hooft, Nucl. Phys. **B61**, 455 (1973).

[31] W. Marciano, Phys. Rev. D **29**, 580 (1984).

[32] A. Giveon, L. J. Hall, and U. Sarid, Phys. Lett. B **271**, 138 (1991).

[33] H. E. Haber and R. Hempfling, Santa Cruz Report No. SCIPP-91/33, 1992 (unpublished).

[34] S. Weinberg, Phys. Lett. **91B**, 51 (1980).

[35] L. J. Hall, Nucl. Phys. **B178**, 75 (1981).

[36] R. Barbieri and L. J. Hall, Phys. Rev. Lett. **68**, 752 (1992).

[37] K. Hagiwara and Y. Yamada, Report No. KEK-TH-331, 1992 (unpublished); A. E. Faraggi, B. Grinstein, and S. Meshkov, SSCL Report No. 126, 1992 (unpublished).

[38] O. V. Tarasov, A. A. Vladimirov, and A. Y. Zharkov, Phys. Lett. **93B**, 429 (1980); S. G. Gorishny, A. L. Kateav, and S. A. Larin, Yad. Fiz. **40**, 517 (1984) [Sov. J. Nucl. Phys. **40**, 329 (1984)]; S. G. Gorishny *et al.*, Mod. Phys. Lett. A **5**, 2703 (1990).

[39] R. Tarrach, Nucl. Phys. **B183**, 384 (1981).

[40] In the notation of Ref. [6] these parameters are $y^{-1} = [\lambda_t(M_G)/\lambda_t]^{1/6}\eta^{1/12}$. In the notation of Ref. [7], $y = \xi$ and $x = (\gamma_D/\gamma_E)^{-1}\eta^{1/2}$.

[41] J. Gasser and H. Leutwyler, Phys. Rep. **87**, 77 (1982). Referred to as GL in the text.

[42] G. Anderson, S. Raby, S. Dimopoulos, and L. J. Hall, Ohio State Report No. OHSTPY-HEP-92-018, 1992 (unpublished).

[43] E. Ma and S. Pakvasa, Phys. Lett. **86B**, 43 (1979); Phys. Rev. D **20**, 2899 (1979); K. Sasaki, Z. Phys. C **32**, 149 (1986); B. Grzadkowski and M. Lindner, Phys. Lett. B **193**, 71 (1987); M. Olechowski and S. Pokorski, *ibid.* **257**, 388 (1991).

[44] K. S. Babu, Z. Phys. C **35**, 69 (1987); B. Grzadkowski and M. Lindner, Phys. Lett. B **198**, 64 (1987); see also the last paper of Ref. [43].

[45] CERN library integration routine DDEQMR based on the algorithm in N. Lance, *Numerical Methods for High Speed Computers* (Iliffe and Sons, London, 1960), p. 56.

[46] V. Barger, M. S. Berger, A. L. Stange, and R. J. N. Phillips, Phys. Rev. D **45**, 4128 (1992); V. Barger, K. Cheung, A. L. Stange, and R. J. N. Phillips, Phys. Rev. D **47**, 4914 (1992); *ibid.* (to be published); H. Baer, M. Bisset, C. Kao, and X. Tata, Phys. Rev. D **46**, 1067 (1992); J. F. Gunion, R. Bork, H. E. Haber, and A. Seiden, *ibid.* **46**, 2040 (1992); J. F. Gunion, H. E. Haber, and C. Kao, *ibid.* **46**, 2907 (1992); J. F. Gunion and L. H. Orr, *ibid.* **46**, 2052 (1992); Report No. UCD-91-10, 1991 (unpublished); H. E. Haber, R. Hempfling, and Y. Nir, Phys. Rev. D **46**, 3015 (1992); Z. Kunszt and F. Zwirner, Nucl. Phys. **B385**, 3 (1992).

[47] B. Ananthanarayan, G. Lazarides, and Q. Shafi, Phys. Rev. D **44**, 1613 (1991).

[48] S. Dimopoulos, L. J. Hall, and S. Raby, Phys. Rev. D **47**, R4793 (1992); U. Sarid and Y. Nir, Phys. Rev. D (to be published).